SCUOLA DI ALTA FORMAZIONE

DOTTORATO IN BIOTECNOLOGIE PER L'UOMO
DOTTORATO IN MEDICINA CLINICA E SPERIMENTALE
DOTTORATO IN MEDICINA MOLECOLARE

PhD Program in
Biotechnologies for Human Health

Thermo-responsive methylcellulose based hydrogel for regenerative medicine applications

Candidate: Andrea Cochis

Tutor: Prof.ssa Lia Rimondini

Phd coordinator: Prof. Claudio Santoro

2013-2014

Cycle 26°

INDEX.

PREFACE.

Background.

Tissue engineering is a very attractive branch of modern medicine. In fact, it represent not only a promising vehicle to face the "regenerative medicine" requests, but it is also a very sophisticate tool for the *in vitro* studies of complex biological systems such as tissues development and regeneration. A great step forward in tissue engineering advancement is represented by the improvement of biomimetic materials that are able to active interact with cells in order to provide microenvironments suitable for the clinical application and the basic theory progress. From this point of view, hydrogels are nowadays considered as a very interesting materials thanks to their biocompatibility and controllable mechanical features. Their utilization range from the 3D matrix for cells development to the drug delivery systems. Thus, the hydrogel development course is an excellent possibility for the making of a platform for biological and clinical investigations.

Aim and presentation of the Thesis.

In this PhD Thesis, it will be reported the three years activities of the candidate. The main purposes has been the development of a novel hydrogel with thermo-sensitive and thermo-reversible features. After that first crucial step, the selected hydrogel has been tested for biomedical purposes facing different applications. Therefore, the Thesis has been divided into 4 different chapter in order to better detail the succeeding steps that are all related to each others. In turn, each of the 4 chapters is characterized by a specific introduction, materials and methods and results and discussion sections with the purpose to minutely explain the biological hypothesis encountered and the strategies used to face them. As support of the selected techniques, a chapter specific references section was spent to each one.

- In the **Chapter 1**, it will be described the methylcellulose-based (MC) thermo-reversible hydrogel development from a mechanical point of view. The purpose was to select the best salts-MC w/v compositions in order to produce a hydrogel able to reverse the physical phase (from liquid to gelation and vice-versa) at 37°C that is the optimal temperature for cells cultivation. Furthermore, the selected hydrogel cytocompatibility was first verified *in vitro* and then the biocompatibility evaluation was extended to the *in vivo* immunological reaction study. Experimental procedures of this part were performed in the Biomedical Materials Laboratory of the Health Sciences Department in Novara for the biological part and in the Laboratory of Materials Sciences of the Polytechnics of Milan for the mechanical assays part.

- After the MC-hydrogel biocompatibility confirmation, in the **Chapter 2**, it will be showed a first biological application for the *in vitro* production of artificial cartilage. In this section, the MC hydrogel has been used in combination with a porous polyurethane scaffold (PU) as 3D matrix for mesenchymal stem cells (MSCs) chondrogenesis. The MSCs differentiation has been carried out using a specific bioreactor able to promote chondrogenesis by the appliance of compression and shear forces on the PU-hydrogel-MSCs composite. By this way, it was possible to produce artificial cartilage via mechanical stimulation, avoiding the use of biochemical stimulation. The successful results were an important proof of the MC-hydrogel suitability as 3D matrix for cells development. All the experiments were performed in the Musculoskeletal Regeneration Laboratory of the AO Research Institute of Davos Platz (Switzerland) within the COST-NAMABIO exchange program (European grant to the candidate).
- In the **Chapter 3**, it will be described the use of the hydrogel as scaffold for the *in vitro* biofabrication of implantable cell sheets (CS). Therefore, it will be detailed the protocol used to cultivate a monolayer of cells onto the MC-hydrogel surface and the subsequent spontaneous detachment allowed by the hydrogel temperature-guided inversion phase. CS were successfully produced, collected and their ability to adhere to a new substrate was *in vitro* confirmed. Afterwards, CS were in vivo implanted into recipient mice; thanks to the presence of cells natural extracellular matrix (ECM), the CS were able to adhere to the naïve tissue without the use o sutures. The successful implantation was confirmed by the neo-vascularization occurred after 2 weeks. Thus, the suitability of the MC-hydrogel for the biofabrication of implantable CS was confirmed. All the procedures were performed in the Biomedical Material Laboratory.
- Finally, in the **Chapter 4**, it will be detailed the MC-hydrogel derived CS technique application for skin regeneration. For this purpose, a complex system composed of a human recombinant elastin (HELP) layer and gingival derived primary human fibroblasts (HGF) was realized. The HELP-HGF CS was detached from MC-hydrogel surfaces and *in vitro* characterized. Afterwards, HELP-HGF CS were implanted into the dorsal skin of nude mice carry a 1cm diameter skin excision mimicking a 3rd degree burn. The CS were attached by fibrin glue avoiding the use of sutures and after 1and 3 weeks the regenerative potency of the CS was confirmed as a complete repair of the skin excision was noticed. These findings represented a strong proof of the CS technology suitability for soft tissues repair. The experiments were performed in the Biomedical Materials Laboratory, while the HELP were kindly produced and

provided by the Laboratory of Recombinant proteins of the Life Sciences Department of the University of Trieste.

Finally, the candidate declare that all the presented data were original and that all animals surgical procedures were performed after local ethical committee approval, following pre-approved surgical procedures.

Chapter 1.

Thermo-reversible methylcellulose-based Hydrogel production, mechanical characterization and biocompatibility evaluation.

In collaboration with the Polytechnics of Milan.

Laboratory of Materials Engineering

1.1 INTRODUCTION

1.1.1. Hydrogels characteristics.

Between the polymeric materials class, a very interesting role is played by the hydrogels. They can be defined as 3D macromolecular structures able to retain a high amount of solvent thanks to their thermodynamic affinity with it. In fact, hydrogels are composed by complex reticular networks supported by physic, ionic and covalent interactions [1-3]. Therefore, hydrogels present both high-energy (covalent bonds) and low-energy (hydrophobic interactions) crosslinks (Figure 1A). However, it is very important the presence of high-energy covalent bonds between polymer chains since they confer to the hydrogel the ability to absorb the solvent without losing their macromolecular integrity (Figure 1B) [2].

Hydrogels can be composed by a multiple repetition of a single polymer (homopolymer) or by the presence of different polymers (copolymer); moreover, it is possible to distinguish between hydrogels presenting a random polymer chains network (amorphous), a partly ordered network (semi-crystalline) or a complete ordered network (crystalline) [4, 5].

Another important hydrogels peculiarity is related to the chemical groups that strongly condition the ionic charge. From this point of view, it is possible to divide hydrogels in neutral (no charge), positive/negative charged (presenting a prevailing $^{(+)}$ or $^{(-)}$ charge) or ampholytes when they have the ability to act both as positive or negative charged responding to an environmental stimulus. Neutral hydrogels develop a complex 3D structure thanks to the energy balance between the solvent osmotic force and the deformation energy of the polymer chains network. In the case of charged hydrogels, the ability to absorb solvent is mainly leaded by two driven forces: the electrostatic repulsion between the polymer chains charges and the osmotic force derived by the presence of charges into the solvent-polymer solution [4, 5].

1.1.2. Hydrogels as *smart* materials.

A novel interesting class of materials suitable for biomedical applications consists on the "*smart*" materials. These particular polymers are able to range their physical/chemical properties following an external stimulus such as pH or temperature changing [6-9] (Figure 1C). Some hydrogels belong to this peculiar order of materials. In fact, they present two distinct phases (Figure 1B): in the (I) collapsed phase, the hydration solvent is repulsed since the interactions energy between the polymer chains are predominant to the solvent-polymer ones. In the (II) swollen phase, the hydration solvent is absorbed because the polymer chains-hydration solvent become predominant to the chains-chains ones [7]. The passage from a collapsed to a swollen state correspond to a physical change of the

hydrogel from a liquid phase, in which the polymer is solved, to a gel phase. In the gel phase, the hydrogel finally tend to jellify because of the polymer chains network reticulation.

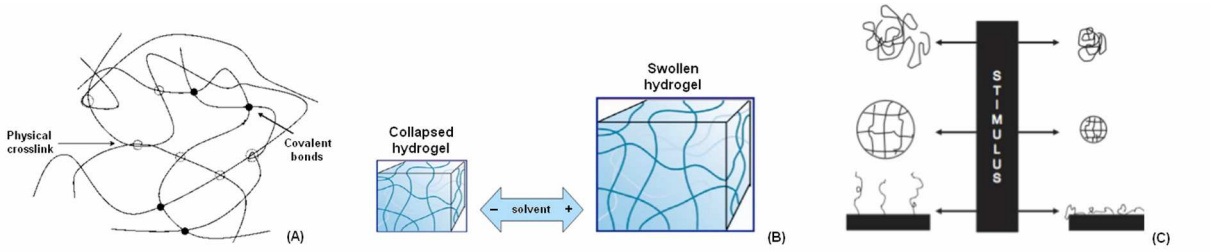

Figure 1 A-C. Schematic representation of the low/high energy network supporting hydrogel macromolecular structure (A). Hydrogel ability to absorb solvent without losing the polymer chains crosslink (B). Smart materials are able to vary their chemical/physical phase following an external stimuli (C).
(A=modified from [3], B=modified from [6], C=modified from [9])

1.1.3. Methylcellulose-derived thermo-reversible hydrogels.

Methylcellulose (MC) is commonly derived from cellulose by the substitution of hydroxyl groups (-OH) with methoxy groups ($-OCH_3$) in a two-steps process involving first sodium hydroxide and then methyl chloride [10]. At the end of the process, MC achieve a structure characterized by the presence of both hydrophilic (-OH) and hydrophobic ($-OCH_3$) groups (Figure 2A). Accordingly, the MC phase in solution is directly determined by the system temperature (T) [10-11]. In fact, when T>55°C MC became not solvable due to the prevalence of the polymer chains hydrophobic interactions; on the opposite, when T<20°C MC results as solvable as the hydrophilic interactions between solvent and polymer chains are predominant on the hydrophobic ones. So, by mixing the MC powder in a defined weight/volume (w/v) percentage in a solvent, it is possible to obtain *smart* hydrogels that are able to undergo a solution-gelation (sol-gel) phase change guided by the system temperature [12-14].

The presence of salts in the hydrogels hydration solvent (that is normally water) is very useful to improve the stability of the hydrogel and it is also a tool to determine the decrease of the phase-changing temperature. In fact, when the T is raised, the system tend to absorb the heat and to convert it into the energy necessary to originate the MC chains-chains crosslink. The water molecules tend to accumulate close to the salts reducing the total number of hydrophilic interactions. Therefore, the energy that is necessary to broke these hydrophilic interactions and undergo MC chains-chains crosslink is lower and the system T for the phase-change decrease (Figure 2B) [12-14].

As in the presence of salts the system sol-gel phase transition is more easy controlled and require lower T, it is very important to underline that this phenomenon results as reversible. Is in fact

possible with MC-based hydrogels to carry out the sol-gel transition and return to the sol phase by lowering the T for a gel-sol phase transition [12].

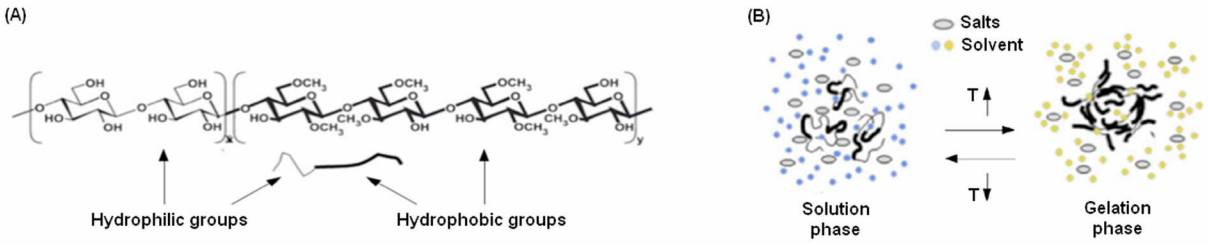

Figure 2 A-B. Methylcellulose chemical structure characterized by the presence of both hydrophilic (left) and hydrophobic (right) groups (A). Representative scheme of the sol-gel phase transition of MC-based hydrogels in the presence of salts and solvent (B).
(Modified from [4])

In conclusion, it is possible to consider the MC-based hydrogel as a *smart* thermo-reversible material sensitive to the system temperature.

1.1.4. Aim of the work.

In this first part of the Thesis, thermo-responsive hydrogels composed of MC and different salt solutions were prepared and characterized. Rheological analysis were performed to determine variations of complex viscosity (η*), conservative shear modulus (G') and viscous shear modulus (G") of hydrogels after temperature increase. The thermo-reversible features of MC-based hydrogels was also investigated by the inversion test and rheological characterization. Selected prepared MC-based hydrogels were preliminary *in vitro* tested to investigated possible cytotoxicity towards mouse fibroblasts. Afterwards, gel-phase MC hydrogels biocompatibility were *in vivo* evaluated into wild type mice.

1.2. MATERIALS and METHODS.

1.2.1. Materials.

Methylcellulose (MC, Methocel A4M, η =4000 mPa×s for a 2% w/v aqueous solution at 20°C) was kindly supplied by The Dow Chemical Company. All basic chemicals were obtained from Sigma-Aldrich unless mentioned otherwise.

1.2.2. Thermo-reversible MC-based hydrogel preparation.

Aqueous MC solutions in different concentrations (Table 1) were prepared with the addition of selected salts (sodium sulphate, Na_2SO_4, sodium phosphate, Na_3PO_4, calcium chloride, $CaCl_2$) or

Phosphate Buffered Saline (PBS), varying their concentration in the MC solution (Table 1).

Salt	Salt concentration	Salt abbreviation
Na_2SO_4	0.02 M - 0.05 M - 0.07 M - 0.1 M - 0.2 M	SO
Na_2PO_4	0.1 M - 0.2 M – 0.3 M – 0.4 M	PO
$CaCl_2$	0.05M - 0.1 M - 0.2 M	CI
PBS	5 g/l - 10 g/l - 50 g/l	PBS
MC concentration [% w/v]	2 - 4 – 6 - 8 - 10 - 12	

Table 1. Salts and MC concentrations for the hydrogels production

MC concentration / salt concentration	2% w/v	4% w/v	6% w/v	8% w/v	10% w/v	12% w/v
0.02 M					Na_2SO_4	Na_2SO_4
0.05 M				Na_2SO_4	Na_2SO_4 $CaCl_2$	Na_2SO_4 $CaCl_2$
0.07 M				Na_2SO_4		Na_2SO_4
0.1 M		Na_2SO_4	$CaCl_2$	Na_2SO_4 $CaCl_2$	Na_2SO_4 $CaCl_2$	Na_2SO_4 $CaCl_2$
0.2 M		Na_2SO_4	$CaCl_2$	$CaCl_2$	Na_2SO_4 $CaCl_2$	$CaCl_2$
5 g/l		PBS		PBS	PBS	PBS
10 g/l	PBS	PBS		PBS	PBS	PBS
50 g/l	PBS	PBS		PBS	PBS	

Table 2. Prepared MC hydrogels; on the row the salt concentration and the PBS concentration are reported, on the columns the MC concentration.

In the following, the composition of the prepared and characterized MC hydrogels will be summarized by acronyms in which the first number is referred to the MC concentration (% w/v), the letters indicate the salt and the last number is referred to the salt or PBS concentration (moles/l for salts, g/l for PBS). The preparation of the MC hydrogels consisted in three main steps, as reported in Figure 3A: 1) preparation of the saline solution; 2) addition of the MC to the saline solution; 3) hydration of the MC powder (i.e. sol phase).

Step 1: preparation of saline solution: saline solutions were prepared mixing the appropriate quantity of the salt with distilled water or PBS (Table 1) at 50°C under magnetic stirring.

Step 2: mixing: the MC was added to the saline solution under stirring at 50°C using the dispersion technique [15], to allow a homogenous distribution of the MC powder in the solution. The MC suspension was poured in tissue culture polystyrene Petri dishes or in the wells of TCPS multi-well plate.

Step 3: MC suspension hydration: to allow the complete hydration of the MC powder, after the mixing step, the suspension was cooled down to 4°C. At 30-35°C, depending on the MC hydrogel composition, MC powder started to hydrate and the viscosity of the solution increased (gel phase). The prepared MC solutions (Table 2) were then stored at 4°C overnight to allow the complete hydration of the MC powder, thus obtaining the hydrogel in the sol phase.

1.2.3. Gelation test.

The physical gelation of MC hydrogels was observed visually using the inversion method already described in literature [13, 15]. Briefly, specimens (10 ml each, n=3) of MC hydrogels (Table 2) were put in different Falcon tubes (15 ml), and heated up to 40°C in a standard bath. Temperature was then decreased down to 20°C, at approximately 0.5°C/min. At 37 and 20°C, the Falcon tube

was inclined of 90° and the possible flow of the MC solution was observed. At each temperature, the solutions/gels were allowed to equilibrate for 1 h. The gelation criterion was defined as the temperature at which the clear solution did not flow upon inversion of the Falcon tube [b].

1.2.4. Rheological characterization.

Rheological characterization of MC hydrogels was performed with a rotational rheometer (AR-1500ex, TA Instruments, USA), using a flat plate geometry (diameter=2 cm, working gap=1 mm). A home-made isolation chamber in polymethyl methacrilate (Plasting srl, Segrate, MI, IT) was designed and assembled to the rheometer to prevent the possible dehydration of the MC hydrogels during the test. Tests were performed using five samples for each considered MC hydrogel composition. To investigate the rheological properties of the MC hydrogels, dynamic viscosity (η*), storage shear modulus (G') and viscous shear modulus (G") were registered over the temperature range 5-50°C, with a temperature ramp of 5°C/min. The oscillation frequency during the temperature ramp was held at 1 Hz. Thermo-reversibility characteristic of the MC hydrogels was studied with a first run increasing the temperature from 4 up to 40°C and a second run decreasing the temperature down to 4°C (temperature ramp=10°C/min, oscillation frequency=1 Hz).

1.2.5. *In vitro* cytotoxicity evaluation.

In vitro cytotoxicity of the MC hydrogel extracts was assessed using murine fibroblasts (L929, ECACC No. 85011425). The hydrogels with the highest salt concentration (Table 3) were prepared under laminar hood using saline solutions previously sterilized with antibacterial filter (Minisart 20 nm, Sartorius Stedim Biotech). Then, the obtained hydrogels were sterilized by UV light exposure (t=30 min). L929 fibroblasts were cultivated in Dulbecco's Modified Eagle's Medium (DMEM, Sigma-Aldrich) supplemented with 10% foetal bovine serum (Sigma) and 1% penicillin/streptomycin at 37°C, 5% CO_2; when cells reached 80-90% confluence, they were detached by trypsin-EDTA solution, harvested and used for experiments. Cylindrical (diameter=10 mm, thickness=3 mm, n=3) samples of different considered hydrogels compositions (Table 3) were put into the wells of a 24 TCPS multiwell plate (CellStar, VWR-PBI International) and submerged for 1 week with 2 ml of complete medium.

	Salt	Salt concentration	MC concentration
4SO0.2	Na_2SO_4	0.2 M	4% w/v
4Cl0.2	$CaCl_2$	0.2 M	
4PBS50	PBS	50 g/l	

Table 3. MC hydrogels investigated in the in vitro cytotoxicity test

Afterwards, surnatants were collected from different samples and used to cultivate cells (cell density=1 x 10^4 cells/well, cell suspension=500

µl/well) for 24, 48 and 72 h. At each time-point, cells viability was evaluated by the (3-(4,5-Dimethylthiazol-2-yl)-2,5-diphenyltetrazolium bromide) colorimetric metabolic assay (MTT, Sigma). Briefly, 50 µl of MTT solution (3 mg/ml in PBS) were added to each well and incubated for 4 h in the dark. Then, surnatants were removed, formazan crystals were dissolved with 100 µl of dimethyl sulphoxyhde (DMSO), and 50 µl were spotted into a 96 TCPS multiwell plate. Sample optical density (O.D.) was evaluated by spectrophotometer (SpectraCount, Packard Bell) at 570 nm. Cells cultivated with fresh DMEM were used as positive control and their O.D. was considered as 100% viability. Furthermore, cells morphology was observed 72 h after seeding by light microscope (Leica AF6500, Leica Instruments). Experiments were performed 3 times using triplicates.

1.2.6. *In vivo* biocompatibility evaluation.

Considering the mechanical assays results and the promising cytocompatibility evaluation data, the 8% w/v Na_2SO_4 0.05M was selected as the best composition for further in vivo biocompatibility investigations. One centimetre diameter specimens of the selected hydrogel were subcutaneously implanted into a pocket realized in the dorsal skin of 6-8 weeks old mice (C57BL/6JOlaHsd, wild type, Harlan Laboratories) (Figure 8 A-B). After 1, 3 and 6 weeks cellular immune responses were determined by using a lymphocyte proliferation assay in tissue culture wells [16]. Spleens were harvested and single cell suspensions prepared by tissue disruption. Lymphocytes were washed, counted, and assessed for viability in trypan blue counting fluid, and adjusted to a suspension of 2.5×10^6 cells/mL in Minimal Essential Medium Alpha modification (α-MEM, Sigma) supplemented with 10% FBS, 1% antibiotics. Triplicate aliquots were dispensed in wells previously coated with 100µl of hydrogel solution or buffer alone. Positive controls consisted of cells stimulated with the mitogen ConA (5 mg/mL) in additional wells to confirm that they were competent. Plates were incubated at 37°C, 5% CO_2 for 48 hours. Cells viability was evaluated by the MTT assay and the cellular responses were expressed as stimulation indices (SI) calculated according to the formula: [(Mean OD of cells cultured with hydrogel - Mean OD of cells cultured without hydrogel) / Mean OD of cells cultured without hydrogel] x 100 [16].

1.2.7. Statistical analysis of data.

Results are expressed as mean and standard deviation. Data, where possible, were statistically compared by a t-test (Student test) or a One-Way ANOVA test (significance level p=0.05), using Bonferroni test for mean comparison (8.5 software).

1.3. RESULTS and DISCUSSION.

1.3.1. Gelation test.

All the compositions of MC blended with saline solution changed from a clear solution at lower temperature (sol phase) to an opaque gel (gel phase) at elevated temperature (T ≥ 37°C). As a representative example (Fig. 3B), the 4SO0.2 hydrogel appears as a clear solution (sol phase, Fig. 3B, left panel) at low temperature (T = 4°C), then the gelation of the solution becomes evident by the opacity of the formed gel up to 37°C (gel phase, Fig.3B, right panel). The inversion test performed for all the investigated compositions (Table 2) evidenced the influence on the gelation temperature of the MC and the salt concentration (Fig. 4). In general, hydrogels obtained using high MC concentration showed a slower flow rate for the higher viscosity. On the contrary, hydrogels with low MC concentration showed a lower viscosity, hence flowed faster. Besides, at the same concentration of MC, different gelation temperature can be detected varying the salt (Fig. 4A). In particular, comparing 4SO0.1 and 4PBS10, a higher gelation temperature value was found for the hydrogel prepared with PBS. For the 8% w/v MC concentration, no correlation with type of salt was evidenced. Considering higher MC concentration, PBS and Na_2SO_4 showed the same low gelation temperature (T=20°C), instead, the gel prepared with $CaCl_2$ maintained a higher gelation temperature (T=37°C). For all the investigated salts (Fig. 4B) and PBS (Fig. 4C) concentrations blended with MC, a decrease in the gelation temperature below 37°C was observed increasing the salt concentration. In addition, the limit salt concentration value, corresponding to the gelation temperature of 37°C, is not the same for all the investigated salt. This is due to a different ionic interaction between the salt ion and the MC. As an example, for 10SOx and 12SOx the limit concentration is 0.05 M, while for 12Clx is 0.1 M. Moreover, for PBS, the limit concentration is 10 g/l for 2PBSx and 8PBSx, while for 10PBSx and 12PBSx corresponds to 5g/l. These qualitative data indicated that the temperature at which the gelation starts can be varied by changing either the MC concentration and the formulation of the saline solution.

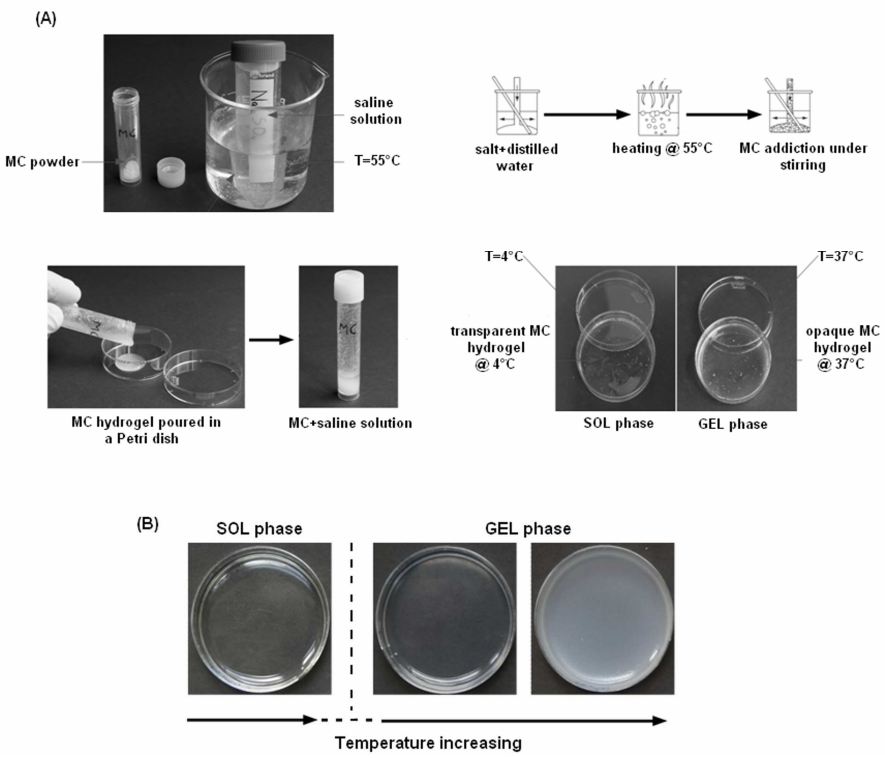

Figure 3 A-B. Schematic representation of the 3-steps hydrogel production process (A). Example of a sol-gel phase transition of a hydrogel spotted into a Petri dish (B).

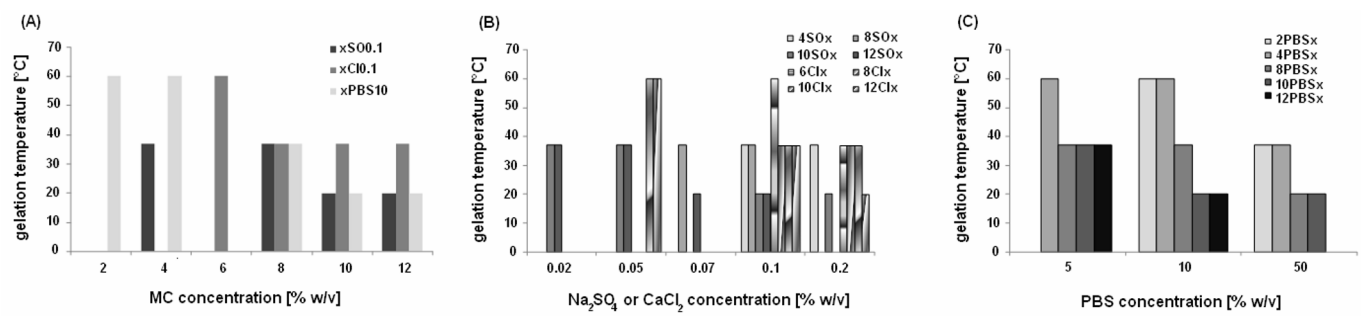

Figure 4 A-C. Gelation temperature of MC blended with salt: (A) effect of concentration of MC blended with 0.1 M Na_2SO_4 or $CaCl_2$, or 10 g/l PBS; (B) effect of Na_2SO_4 or $CaCl_2$ concentration; (C) effect of PBS concentration. (x indicates the different MC concentration in the hydrogel).

1.3.2. Rheological characterization.

In Figure 5, the storage shear modulus (G') and the loss shear modulus (G'') obtained from the temperature sweep rheological analysis are reported for the compositions that showed a gelation temperature about 37°C in the inversion test. In fact, this value appears the optimal one for a possible use as smart hydrogel in regenerative tissue applications. For all the selected MC solutions, at low temperature (approximately in the range 5-10°C), G' (Fig. 5 A-C) was lower than G'' (Fig. 5

D-F) due to the viscous/liquid-like behavior of the MC solution, i.e. sol phase. Increasing the temperature, G' first showed a decrease, reaching a minimum, then it rapidly increased for the sol/gel transition, as a soft elastic gel is formed. In addition, increasing the MC concentration higher values of G' can be detected. Besides, increasing the salt concentration, at the same MC concentration, G' increased and a slight shifting towards lower temperature (T<37°C) was evidenced for the gelation temperature, confirming the inversion test results.

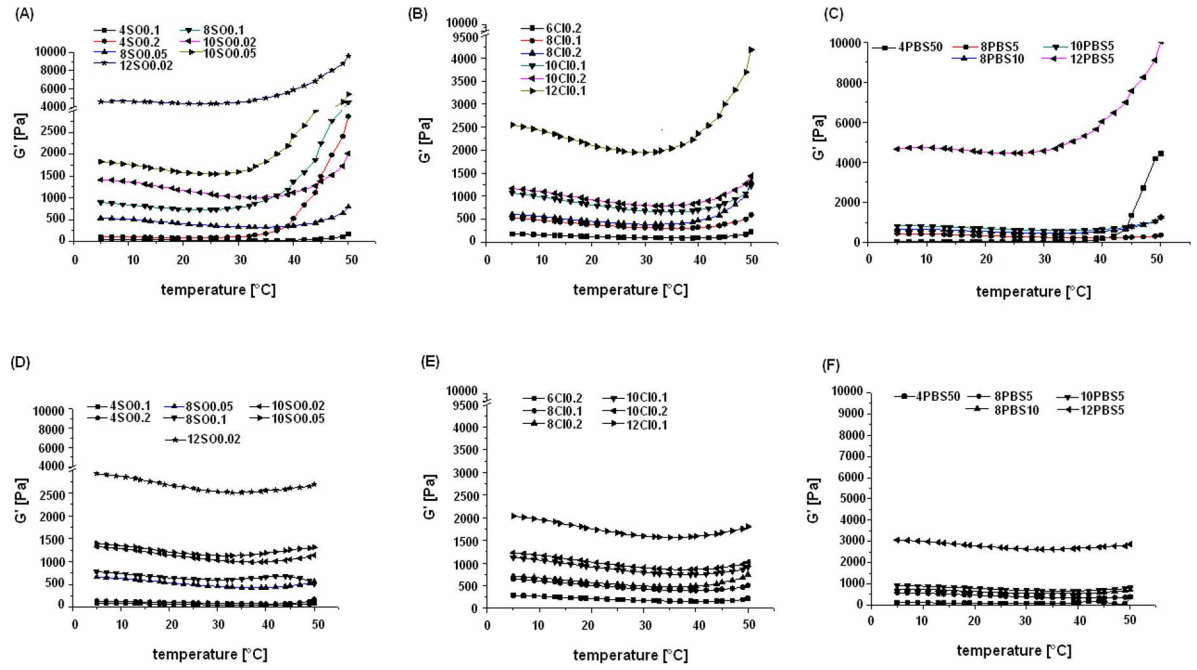

Figure 5 A-F. Shear storage modulus (G') and shear loss modulus (G'') versus temperature for the solutions prepared varying MC and salt concentration: A-D) MC blended with Na_2SO_4; B-E) MC blended with $CaCl_2$; C-F) MC blended with PBS. Curves represent the average behavior of G' ad G'' obtained by the rheological data collected at every 0.5°C temperature interval at a frequency of 1 Hz.

In the heating and cooling tests (Fig. 6), a hysteresis is observed for all the investigated solutions. In particular, a higher hysteresis is detected when MC concentration increases for MC blended with salts (Fig. 6A, e.g. 12SO0.02, 8SO0.1, Fig. 6B, e.g. 10Cl0.2, Fig. 6C, e.g. 12PBS5). The high hysteresis detected for some MC compositions could suggest that the solution did not reach the thermal equilibrium in the gelled state and that the dissociation in the MC gel-sol transition (during the cooling run) is not an exact reversal of the association process (during the heating run) [17].

MC based hydrogels prepared in this work exhibited reversible thermo-responsive properties. Phase transition was confirmed both by physical and rheological characterizations. Interesting, it was easily observed how temperature determined variations to hydrogel mechanical properties. When samples were heated, mechanical parameters increased confirming that polymer structure became

more and more ordinate and compact. Conversely, immediately after cooling down temperature, samples showed a decreasing of mechanical parameters which indicated that polymers were losing their compact structure to come back to the liquid phase. These properties are certainly related with MC chemical structure. In fact, it is characterized by the presence of both hydrophobic and hydrophilic groups. Methoxy groups (-CH_3) represent the hydrophobic regions while hydroxy groups (-OH) represent the hydrophilic ones. At low temperature (< 10ºC) hydrophilic interactions between –OH groups and solvent are predominant so MC molecules are hydrated and the polymer structure is held together by simple entanglements. As temperature increase, hydrogels absorb energy and gradually lose their hydration water. Polymer-polymer interactions take place between –CH_3 groups, forming a gel-network structure.

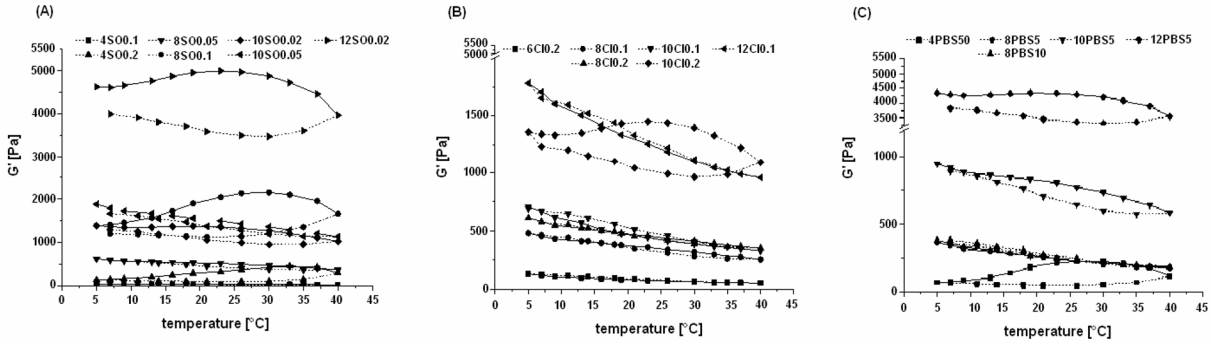

Figure 6 A-C. Temperature dependence of the shear storage modulus (G') for the solution prepared varying either MC and salt concentration: A) MC blended with Na_2SO_4; B) MC blended with $CaCl_2$; C) MC blended with PBS. Straight curves represent the average behavior of G' during the heating up to 40°C, the dash curves during the cooling down to 5°C.

Rheological characterizations showed that MC and salts concentration strongly influenced hydrogels mechanical properties. In fact, the increasing of MC and salts concentration determined an increasing in mechanical parameters. Those are expected results because by adding more MC the final polymer will be composed by a higher number of hydrophobic regions that will form a more structured and compact gel-network. Increasing salts concentration, water molecules are forced to locate around them, reducing the intermolecular hydrogen-bond formation between water molecules and the hydroxyl groups of MC. Not only concentration but also the type of salts strongly influenced hydrogels mechanical properties. In fact usually salts have greater affinity for water than polymers molecules resulting from removing hydration water from the polymer and thus dehydrating the polymer. This phenomena is termed "salt-out" (or salt-assisted) effect and means that water is dropped out from polymer structure [4, 5, 14].

The ability of a salt to salt-out a polymer generally follows the salts order in the lyotropic series [14]. Cations follow the order Li+ > Na+ > K+ > Mg_2+ > Ca_2+ > Ba_2^+, and more common anions

follow the order CNS- < I- < Br- < NO_3^- <Cl- < tartrate < SO_4^{2-} < PO_4^{3-} [14]. These effects depend mostly on the anions. Accordingly, with the same MC and salts concentrations, more water molecules were removed from MC hydrogels when Na_2SO_4 was used than $CaCl_2$.

Evaluating G' and η* values obtained during cooling down phase, it was noticed that they were higher than heating ones. In contrast to the sharp increase of both the parameters from the heating process in the temperature range from 30 to 40°C, the gradual decrease of the parameters with temperature in the cooling process showed an outstanding deviation from the heating curve. This clearly indicates that the thermally induced hydrophobic dissociation is not an exact reversal of the hydrophobic association in the heating process. The hysteresis between the heating and cooling processes may be due to the existence of some associated aggregates or weak connections that have not completely disassociated [17]. Differences may be also due to a different dynamic in forming and destruction of the chain to chain interactions related to the different dynamic in absorbing and realising water. Only under 7ºC the values became again comparable.

Another factor that may affect the destruction of the polymeric structure is the time for which the system has equilibrated at the highest temperature before cooling. In this work, cooling process initiated immediately after the heating process. However, if the sample is allowed to equilibrate for some time before cooling starts, the time should have effect on the hydrogels behaviour during cooling process. Samples should be more difficult to dissociate because of the more perfect network formed, compared to a freshly formed gel at the same temperature and a different trend should be recorded. The aforementioned results indicated that the temperature at which gelation is initiated and the mechanical proprieties can be altered by the concentration of MC and the formulation of the aqueous solvent. In addition, MC hydrogel's composition can be easily manipulated to obtain specific physic-chemical behaviours for different use.

1.3.3. *In vitro* cytotoxicity evaluation.

In vitro cytotoxicity tests were performed on extracts of complete medium previously put in contact with 4SO0.2, 4Cl0.2, and 4PBS50 MC hydrogels for 7 days in order to exclude the release of toxic compounds. These hydrogels have been selected for the *in vitro* test for their higher content of salt used in the preparation of the hydrogels. In fact, a possible cytotoxic effect would be more evident for these hydrogels compared to the ones with a lower salt concentration. The MTT assay showed at each considered time-point (Fig. 7A), no cytotoxic effect caused by the possible release of toxic compounds from the tested MC hydrogels. Indeed, cells viability resulted in a range of 94-99% comparable to the control values for all the time-points with no significant statistically differences

(p>0.05) between the controls and the eluates. Besides, MTT results were also supported by the light microscopy observation (Fig. 7B). Cells cultivated for 72 h in contact with the MC hydrogel eluates showed a morphology, spread and density comparable when seeded in presence of the tested eluates and in fresh medium, confirming that no toxic compounds were released into the culture medium.

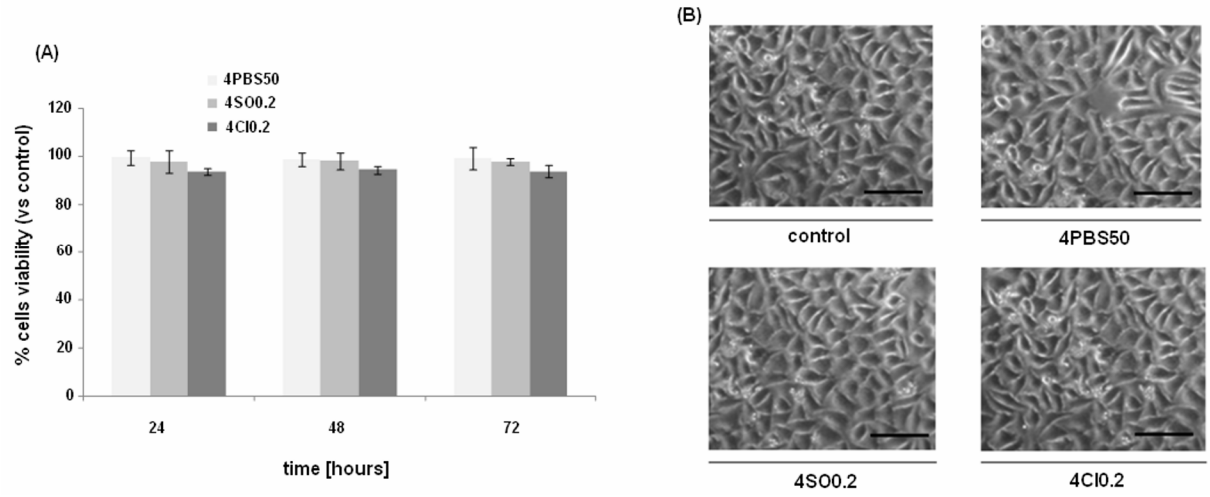

Figure 7 A-B. *In vitro* cytotoxicity evaluation results. (A) Cells viability after 24, 48 and 72 h after seeding in contact with hydrogel eluates; at each time-point, viability values were comparable between control and tested samples and no statistically significant differences were noticed (p>0.05); (B) optical microscopy images of L929 cells 72 h after seeding in contact with hydrogel eluates; a comparable cell morphology, spread and density was observed, supporting cell viability assay results. Bars represent means and standard deviations; bar scale = 200 μm.

According to the *in vitro* preliminary biological characterization results, the selected MC hydrogels showed to be not cytotoxic for mouse fibroblasts. In fact, the viability of cells cultivated in medium previously put in contact with the different hydrogels was comparable to the results obtained for cells cultivated with fresh medium. These data suggest that up to 7 days of hydrogel-medium direct contact, no toxic products were released into the medium. Since the hydrogels containing the highest amount of salts were tested, these findings could be extended also to the other compositions containing a lower salt amount. Besides, MC itself could not be considered as a possible source of toxicity since the one selected is a commercial MC powder largely used for different purposes such as for the food industry and it is well established its cytocompatibility.

1.3.4. *In vivo* immune response evaluation.

Mice implanted with hydrogel did not reported any macroscopic inflammatory reactions such as fibrosis (data not shown) also after a long period after operations. The collected spleens were comparable between control and hydrogel implanted mice (Figure 8 C) revealing the absence of macroscopic evidences of inflammatory processes. When the SI index was calculated at each time-

point, the hydrogel-coated samples score was always < 1 confirming that no inflammatory reactions were raised toward hydrogel. On the opposite, lymphocytes stimulated with the mitogen conA fast reacted reporting SI score always > 1. After 1, 3 and 6 weeks after hydrogel specimens implantation, comparing the SI scores, a statistical significant differences was always noticed between hydrogel and conA groups (Figure 8 D). These findings suggest that the collected primary lymphocytes were competent but reactive towards hydrogel, confirming the polymer biocompatibility.

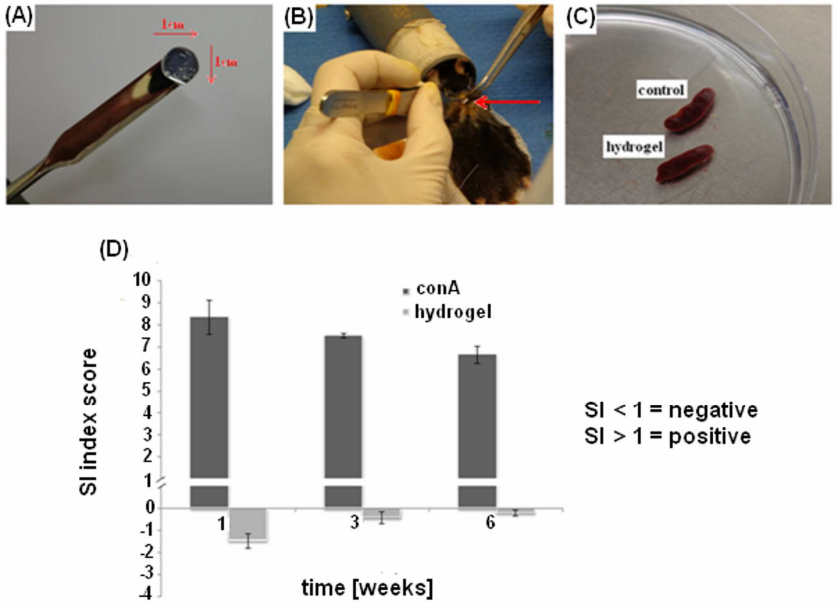

Figure 8 A-D. In vivo immunological reaction. Hydrogel cylindrical samples (A) were implanted in a subcutaneous pocket realized in the mice dorsal skin (B); at each time-point spleens resulted as comparable with controls (C, representative for the 6 weeks) and the SI index revealed that no immune reaction was caused by the hydrogel implants (D) whereas lymphocytes reacted towards conA (D). Bars represent means and standard deviations.

1.4. CONCLUSIONS.

Capitolo 1 In the first part of the Thesis, the salt concentrations were selected to investigate the influence on MC-hydrogels properties, in particular focusing on the thermo-reversible characteristic. It has been demonstrate that some of the prepared MC hydrogels have not only thermo-responsive properties but also reversible thermo-responsive properties. Preliminary in vitro cytotoxicity assay confirmed that hydrogels were compatible with mouse fibroblasts and no toxic compounds were released from them. Between the different tested compositions, the 8% MC Na_2SO_4 0.05M was selected and used for in vivo biocompatibility evaluation. The very encouraging results obtained with the biocompatibility evaluation suggest that the selected hydrogels represent a

very promising materials for biomedical applications.

Acknowledgments.

A. Cochis would like to thanks Dr. Andrea Carletta for the excellent technical support for the hydrogel preparation protocol development. Thanks to Dr. Elena Varoni for the help for the in vivo surgical procedures. A special thanks to Prof. Silvia Farè and Dr. Lina Altomare from the Polytechnics of Milan for their fundamental help in the mechanical tests accomplishment.

References.

1. Peppas NA. Hydrogels, biomaterial science: an introduction to materials in medicine. 2004;100-107.
2. Berger J, Reist M, Mayer JM, et al. Structure and interactions in covalently and ionically crosslinked chitosan hydrogels for biomedical applications. Eur J of Pharm Biopharm. 2004;57:19-34.
3. Slaughter BV, Khurshid SS. Hydrogels in regenerative medicine. Adv Mater. 2009;21:3307-29.
4. Chen CH, Tsai CC, Chen W, et al. Novel living cell sheet harvest system composed of thermoreversible methylcellulose hydrogels. Biomacromolecules. 2006;7:736-43.
5. Chen CH, Chang Y, Wang CC, et al. Construction and characterization of fragmented mesenchymal-stem-cell sheets of intramuscular injection. Biomaterials. 2007;28:4643-51.
6. Hoffman AS. Application of “smart polymers” as biomaterials. Biomaterial science: an introduction to materials in medicine. 2004;107-15.
7. Cooper SL, Visser SA, Hergenrother RW, et al. Polymers biomaterial science: An introduction to materials in medicine. 2004; 67-79.
8. Kumar A, Srivastava A, Galaev IY, et al. Smart Polymers: Physical forms and bioengineering applications. Prog Polym Sci. 2007;32:1205-37.
9. Yang J, Yamato M, Shimizu T, et al. Reconstruction of functional tissues with cell sheet engineering. Biomaterials. 2007;28:5033-43.
10. Honeyman J. Recent advances in the chemistry of cellulose and starch. J Polym Sci. 1960;45:552.
11. Endler A, Persson S. Cellulose synthesis in arabidopsis. Molecular Plan. 2011;4:199-211.
12. Xu Y, Li L, Zheng P, et al. Controllable gelation of methylcellulose by salt mixture. Langmuir. 2004;20:6134-38.
13. Liang HF, Hong MH, Ho RM, et al. Novel method using a temperature-sensitive polymer (methylcellulose) to thermally gel aqueous alginate as a pH-sensitive hydrogel. Biomacromolecules. 2004;5:1917-25.
14. Li L, Thangamathesvaran PM, Yuc CY, et al. Gel network structure of methylcellulose in water. Langmuir. 2001;17:8062-68.
15. Tate MC, Shear DA, Hoffman SW, et al. Biocompatibility of methylcellulose-based constructs designed for intracerebral gelation following experimental traumatic brain injury. Biomaterials. 2001;22:1113-23.
16. Vandevord PJ, Matthew H, DeSilva SP, et al. Evaluation of the biocompatibility of a chitosan scaffold in mice. J Biomed Mater Res. 2002;59:585-90.
17. Chatterjee T, Nakatani AI, Adden R, et al. Structure and properties of aqueous methylcellulose gels by small-angle neutron scattering. Biomacromolecules. 2012;13:3355-69.

Chapter 2.

MC hydrogel as 3D matrix for the bioreactor-guided *in vitro* production of artificial cartilage.

In collaboration with AO Research Institute of Davos Platz, Switzerland.

Laboratory of Musculoskeletal Regeneration.

This work was supported by an European COST-NAMABIO grant to A. Cochis for the visiting period in Davos.

2.1 INTRODUCTION.

2.1.1. Mesenchymal stem cells (MSCs) as possible source for cartilage repair.

Cartilage defects present a challenging reconstructive problem due to the tissue's limited intrinsic capacity for self-repair. Currently, the only FDA-approved cellular-based therapy for cartilage defects involves autologous chondrocyte implantation (ACI), in which chondrocytes harvested from low-contact areas are expanded in culture and then re-injected into a defect [1]. This technique has shown promising results in early clinical studies [1], but is restricted by limited expansion of chondrocytes *ex vivo*, difficulty maintaining chondrocyte phenotype *in vitro*, and donor site morbidity [2, 3]. Alternative cellular therapies have turned to progenitor cell populations such as bone marrow derived stem cells (BMSCs), which have the ability to differentiate into several connective tissue cells types, including cartilage [4]. Clinically, autologous BMSCs have been used to repair articular cartilage defects by surgically transplanting collagen-embedded BMSCs [5-7] and by intra-articular injections of BMSCs [8]. Both techniques have yielded promising results with noted improvements in clinical symptoms such as pain and walking ability.

Adipose derived stem cells (ADSCs) have also been investigated as a less invasive source of chondrocyte progenitors that can be differentiated into chondrocytes *in vitro* [9]. Important considerations in this process include the use of appropriate growth factors, primarily those in the TGF-β superfamily [10], as well culture in a 3-dimensional environment by utilizing cellular scaffolds [11]. These preconditioned ADSCs are then capable of forming cartilage tissue *in vivo* [12]. In addition, uninduced ADSCs transplanted into hyaline cartilage defects in patellofemoral joints [13] and ear auricle defects [14] in animals have completely restored the native cartilage structure and fully repaired the defects at six months and three months, respectively.

2.1.2. The influence of mechanical forces into stem cells chondrogenesis.

Mechanical stimuli are of crucial importance for the development and maintenance of articular cartilage. Many forces are involved in the cartilage microenvironment: hydrostatic pressure, tension, compression and shear (Figure 1 A). Studying in vitro models for cartilage regeneration using mesenchymal stem cells (MSCs), it is very interesting to notice how all of these forces are able to shape cells fate when applied. During loading of the joint, water from the synovial fluid is retained within the cartilage matrix by the presence of charged proteoglycans, resulting in increased hydrostatic pressure (HP). The collagen network functions to prevent swelling of the tissue. Experimental studies indicate intermittent application of HP in the physiological range of 7 to 10 MPa over longer time periods promotes matrix synthesis, whereas constant pressure seems

unsuitable [15]. Tensile loading is not generally regarded as physiologically relevant for articular cartilage and has therefore attracted little attention. However, is evidence that articular cartilage in vivo is under a degree of static pretension: therefore, the effect of intermittent static biaxial tensile strains on cartilaginous constructs was studied [16]. Results showed that average magnitudes of 3.8% radial and 2.1% circumferential tensile strains for 30 minutes lead to the greatest increase in proteoglycan content. By far the greatest number of studies involving mechanical load has been performed using bioreactors that apply uniaxial compression. Direct compression results from direct contact between joint surfaces and has been simulated in a diverse number of reactor systems. For articular cartilage of the major weight bearing joints in the hip and the knee, average loadings of approximately 0.5 to 7.7 MPa and average compression amplitudes of more than 13% have been measured during normal daily movements [17]. A wide range of loading frequencies (0.001–5 Hz) and amplitudes has been applied to TE cartilaginous constructs. A number of studies involving dynamic compression suggest a beneficial effect of load for chondrogenesis of MSCs, resulting in an increase in collagen II and aggrecan. Most of these studies used a frequency of 1 Hz and either 10% [18] or 15% [19] compression. These are similar magnitudes to those that lead to the greatest increase in chondrogenic gene expression and GAG synthesis in chondrocytes [20]. Finally, shear stress is a potent modulator of the amount and type of extracellular matrix synthesized, suggesting that the best way to envision the typical loading processes affecting articular cartilage is to recognize them as a rolling movement of direct compression in concert with a generation of shear and tensile forces and high hydrostatic pressure [21].

2.1.3. Bioreactor-guided chondrogenesis.

Many different biomaterial scaffolds have been used to study the effect of dynamic loading on chondrocytes and MSCs. There is a strong dependency of the mechanical signal sensed by the cells on the material mechanical properties as shown by the wide range of compressive load applied. Tailored synthetic crosslinked poly(ethylene glycol) hydrogels have been prepared to study the interactions between chondrocytes and material in compressive static and dynamic culture systems [22]. Over short culture periods, dynamic loading of 15% strain at 1 Hz did not affect considerably the chondrocyte extracellular matrix gene expression (Type I and II collagen and aggrecan) compared with the static mode when encapsulated in a non degradable crosslinked pure poly(ethylene glycol) hydrogel [22]. At first glance, this seems to contradict others' findings that demonstrate the importance of dynamic loading on chondrocyte gene expression and differentiation of MSCs encapsulated in a three-dimensional matrix. However, chondrocytes cultured in a similar

poly(ethylene glycol) hydrogel decorated with RGD peptides, which can act as a binding site for chondrocytes, showed substantial gene expression upregulation under mechanical loading compared with static culture [23]. Even if the presence of RGD peptides is not beneficial to the conservation of chondrocyte gene expression, this demonstrates the importance of the interaction/binding between the encapsulating matrix (ie, poly[ethylene glycol]) and the chondrocytes for conveying mechanical signals [23]. The importance of scaffold binding sites or ‘‘bioactivity’’ to transmit mechanical signals to seeded chondrocytes has also been demonstrated for other matrices [24]. MSC survival and differentiation are markedly dependent on their ability to attach on the substrate they have been seeded on. Therefore, similarly as for chondrocytes, the ability of the cells to bind the material is critical to convey mechanical signals. This is one reason for the frequent use of fibrin gel, a favorable substrate for cell attachment with mechanical properties easily tuned by variation of concentration and gelling mechanism. The effect of the hydrogel stiffness on viability could be clearly demonstrated using fibrin gels of different concentrations [25]. Taken together these data suggest culture in a scaffold material that allows for cell attachment, combined with greater than 10% compression at a frequency of 1 Hz, may be a suitable starting point for the physical stimulation of both MSCs and chondrocytes (Figure 1 B-D).

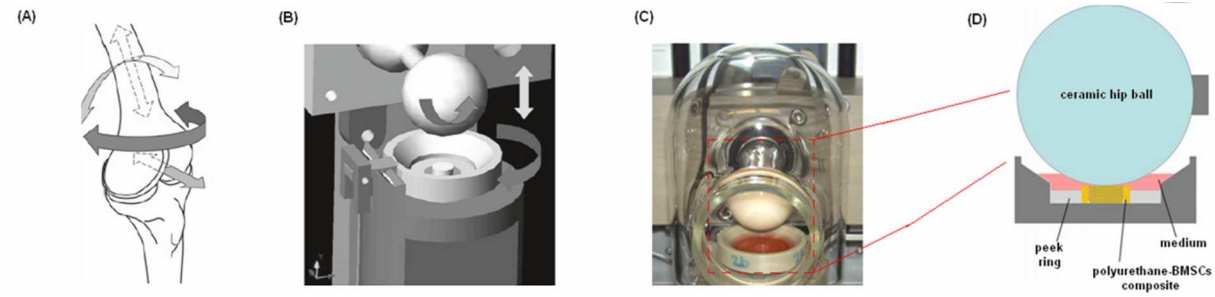

Figure 1 A-D. Schematic showing the directions of movement found within a human knee and (A) the directions of movement that can be applied using a multiaxial bioreactor (B). One of the six stations composing the bioreactor developed by Alini et al. (C) that is featured by a ceramic hip ball that compress and oscillate against a polyurethane-fibrin-BMSCs composite as represented in D.
(Modified from [26])

2.1.4 Aim of the work.

In this second part of the Thesis, the biocompatible MC-based hydrogel was tested as 3D matrix for the bioreactor-guided chondrogenesis of BMSCs. The cells were suspended into the liquid hydrogel that was used to fill a porous polyurethane (PU) scaffold. The PU-hydrogel composite was used for the cells mechanical stimulation exploiting a bioreactor developed by Alini et al. (AO Research Instutite, Davos Platz, Switzerland). This particular bioreactor (Figure 1 B-D) was developed in order to apply with a ceramic hip ball a defined compression and shear force against a porous PU

scaffold (Figure 1 C-D). After a 21 days period of stimulation, BMSCs chondrogenesis was evaluated by PCR and immunohystochemical analysis and the suitability of the MC-based hydrogel as 3D matrix for cells development was verified.

2.2 MATERIALS and METHODS.

2.2.1. Isolation and expansion of human mesenchymal stem cells.

Fresh human bone-marrow aspirates were obtained after full ethical approval (Freiburg, EK-326/08) and informed patient consent. Bone marrow stromal cells were isolated from 4 donors (Male/Female 19-49 years old) by standard density gradient procedure (Histopaque-1077) and selection by plastic adherence. Mesenchymal stromal cells (MSCs) were cultured in polystyrene flasks (TPP) at 37°C, 5% CO_2 (for a 90% humidity atmosphere) in α-modified minimal essential medium (α-MEM, Sigma), 10% human MSC qualified foetal bovine serum (FBS-Hyclone) with 5 ng/mL fibroblast growth factor 2 (HGF, Fitzgerald Industries, Acton, MA, USA). Cells were detached with trypsin-EDTA solution at subconfluence and seeded into the required number of flasks. Thereafter, the medium was changed every 2 days. After the cells reached 70-80% confluence, they were harvested and used for the experiment at passage 2-3. Each experiment was performed separately in quadruplicate for each donor and the data collated for statistics.

2.2.2. Methylcellulose based hydrogel-polyurethane composite culture of MSCs.

Cylindrical (8 mm diameter x 4 mm height) porous polyurethane scaffolds (pore size of 90-300 μm) were prepared as described elsewhere [27]. MSCs were suspended in a 8% w/v methylcellulose (MC) 0.05M Na_2SO_4 based hydrogel before seeding them into the polyurethane scaffolds. Hydrogel was prepared as previously described in Chapter 1; cells were suspended into 160 μl of the liquid hydrogel at a density of 3×10^6 per specimens. Hydrogel containing cells were used to fill the PU scaffold pores by compressing it several times until all the hydrogel was absorbed by PU pores (Figure 2 A-B). Constructs were then incubated for 2 hours at 37°C, 5 % CO_2 and 95 % humidity to allow MC hydrogel transition from gel to solid phase before adding growth medium (DMEM, with 4.5 g/L glucose and 2.2 g/L NaHCO3, non-essential amino acids, containing 11.5 mg/L L-proline (Invitrogen/Life Technologies, Carlsbad, CA, USA), 50 μg/mL ascorbic acid 2-phosphate sesquimagnesium salt hydrate (Sigma-Aldrich, Buchs SG, Switzerland), ITS+1 (10 μg/mL insulin from bovine pancreas, 5.5 μg/mL human transferrin (substantially iron-free), 5 ng/mL sodium selenite, 0.5 mg/mL bovine serum albumin and 4.7 μg/mL linoleic acid; Sigma-Aldrich), 100 U/mL penicillin + 100 μg/mL streptomycin (Invitrogen)). After 2 days of pre-culture in 12-well plates,

constructs were transferred in polyether ether ketone (PEEK) holders. The experiments were carried out at 37°C, 5 % CO_2, 95 % humidity. Medium was changed every 2 days and collected for further analysis.

2.2.3. Bioreactor.

Mechanical conditioning of the cell-scaffold constructs was performed using a pin-on-ball bioreactor system. Briefly, a ceramic ball 32 mm in diameter was pressed onto the scaffold [28]. Interface shear motion was generated by oscillation of the ball about an axis perpendicular to the scaffold axis. Superimposed compressive strain was applied along the cylindrical axis of the scaffold. Samples were exposed to unconfined dynamic compression at 1 Hz with 0.4 mm sinusoidal strain, superimposed on a 0.4 mm static offset strain, resulting in a strain amplitude of 10-20 % of the scaffold height at the centre of the construct. Simultaneously samples were also exposed to ball oscillation of ±25° at 1 Hz, superimposed on a 0.4 mm static compression offset strain. Mechanical load was applied during 1 hour a day for 21 consecutive days over 3 weeks (Figure 2 C-D). Cell-scaffold constructs not loaded into the bioreactor were used as controls. Experiments were carried out in quadruplicate for each donors for both loaded and not loaded samples.

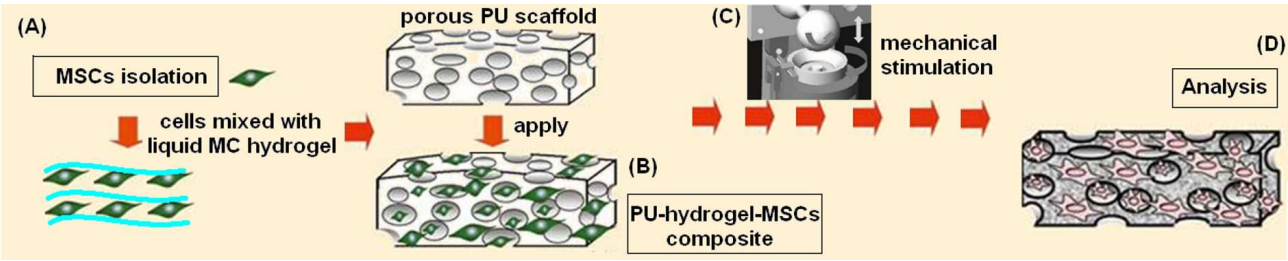

Figure 2 A-D. Schematic representation of the experimental procedures. Stem cells (MSCs) were isolated from human bone marrow, expanded and seeded into the liquid hydrogel (A); afterwards cells-hydrogel solution were used to fill a porous polyurethane (PU) scaffold (B) that was mechanically stimulated for 21 days by bioreactor (C). Finally, scaffolds were collected and used for analysis (D).

2.2.4. Analysis.

After 3 weeks of culture and 21 loading cycles, cells scaffold constructs were vertically cut in two halves; 3 scaffold halves were processed for biochemical analysis, 3 for gene expression analysis and 2 for histological and immuno-hystochemical analysis.

2.2.5. Gene expression.

Scaffolds used for gene expression analysis were homogenized in 1mL TRI reagent and 5µL Polyacryl Carrier (both Molecular Research Center, Cincinnati, OH, USA) per scaffold, using a Tissue-Lyser (Retsch & Co., Haan, Germany) and centrifuged (Eppendorf, Basel, Switzerland) at 4 °C for 10 min at 12000g. RNA isolation was carried out according to the protocol from the manufacturer. RNA was reverse transcribed with TaqMan reverse transcription kit (Applied Biosystems, Foster City, CA, USA) using random hexamers. For real time PCR TaqMan Gene Expression Assays (Applied Biosystems) or custom designed primer-probe sets (from Microsynth, Balgach, Switzerland) were used on a GeneAmp 7500 Real Time PCR System (Applied Biosystems). The endogenous control gene was 18S rRNA. Chondrogenic markers (collagen type-II (Col 2), SRY (sex determining region Y) – box 9 (Sox9), osteogenic marker (collagen type-I (Col 1) and hypertrophic markers (collagen type-X (Col 10)) were analyzed. The primers and probes used are listed in Table 1.

Gene	Abbr.	Primer fw 5' - 3'	Primer rev 5' - 3'	Probe (5' FAM / 3' TAMRA)
Collagen type I	COL 1	CCC TGG AAA GAA TGG AGA TGA T	ACT GAA ACC TCT GTG TCC CTT CA	CGG GCA ATC CTC GAG CAC CCT
Collagen type II	COL 2	GGC AAT AGC AGG TTC ACG TAC A	GAT AAC AGT CTT GCC CCA CTT ACC	CCT GAA GGA TGG CTG CAC GAA ACA TAC
Collagen type X	COL 10	ACG CTG AAC GAT ACC AAA TG	TGC TAT ACC TTT ACT CTT TAT GGT GTA	ACT ACC CAA CAC CAA GAC ACA GTT CTT CAT TCC
Gene	**Abbr.**	**Applied Biosystems Serial number**		
SYR (sex determining region Y) - box 9	SOX 9	Hs_00165814_m1		
18S rRNA	18S	4310893E		

Table 1. Primers / Probes (fw= forward, rv=reverse)

Gene expression was analyzed according to the ΔΔCt method, with expression levels normalized to the corresponding day 0 sample (day of cell seeding into scaffolds) of each donor.

2.2.6. Biochemical analysis.

Scaffolds used for biochemical analysis were digested with 0.5mg/mL proteinase K at 56°C overnight and used for DNA and glycosaminoglycan (GAG) measurement. DNA concentrations were determined with the Hoechst method using calf DNA as a standard. Fluorescence intensity was measured with an HTS 7000 Perkin Elmer Bio Assay Reader (Norwalk, CT, USA). The amount of glycosaminoglycan (GAG) was determined by the dimethylmethylene blue dye method, using bovine chondroitin sulphate as the standard. Proteinase K digests were used to measure the GAG content of the scaffolds. The total GAG content of the culture media, collected every 2 days, was also measured to assess the release of matrix molecules from the sample into the media. Absorbance was measured with a Victor3 Perkin Elmer (Waltham, MA, USA) 1420 multilabel counter. GAG values were normalized to the DNA content.

2.2.7. Histology and Immunohystochemistry.

For immunohystochemical analysis scaffolds were fixed in 70 % methanol at 37°C (to prevent hydrogel solid-gel phase transition) and incubated in 5% D(+) sucrose (Sigma-Aldrich, St. Louis, MO, USA) solution in phosphate buffered saline (PBS, pH 7.4) for 12 h at 37°C before embedding them in Jung tissue freezing compound and cryosectioning at 10μm (Microm HM560 CryoStar, Thermo Scientifi c, Waltham, MA, USA). The presence of glycosaminoglycans (GAG) was investigated by immunohystochemistry using safranin-O GAG specific marker (Sigma). The deposition of collagen types I and II was determined by immunofluorescence staining. After enzyme pre-treatment (0.5 U/mL Hyaluronidase for collagen types I and II staining), sections were blocked with 5% goat serum. Then sections were incubated using primary antibodies raised against collagen I (COL 1, 1:150) and collagen II (COL 2, 1:50). The antibody against type I and II collagen were from Abcam (Abcam, UK). Primary antibody was applied overnight at 4°C; afterwards, sections were washed 3 times with PBS and the appropriate secondary antibody was applied (1:500 in PBS). Samples were visually investigated by fluorescent microscope (Leica DM5500 B, Leica Microsystems, IL, USA).

2.2.8. Statistical analysis.

Statistical analysis was performed using the software package SPSS (Version 20, SPSS Inc, Chigaco, IL, USA). Data were analyzed with Wilcoxon's test. The significance level was defined at $p< 0.05$.

2.3. RESULTS and DISCUSSION.

2.3.1. PCR Analysis.

Polyurethane-hydrogel-MSCs composites gene expression after 21 days of mechanical stimulation with the bioreactor are reported in Figure 3. In general, loaded samples showed a higher expression of the selected genes if compared with the not loaded control ones. Therefore, it is possible to state that the mechanical forces of compression and shear were crucial to affect cells fate during the 21 days of stimulation.

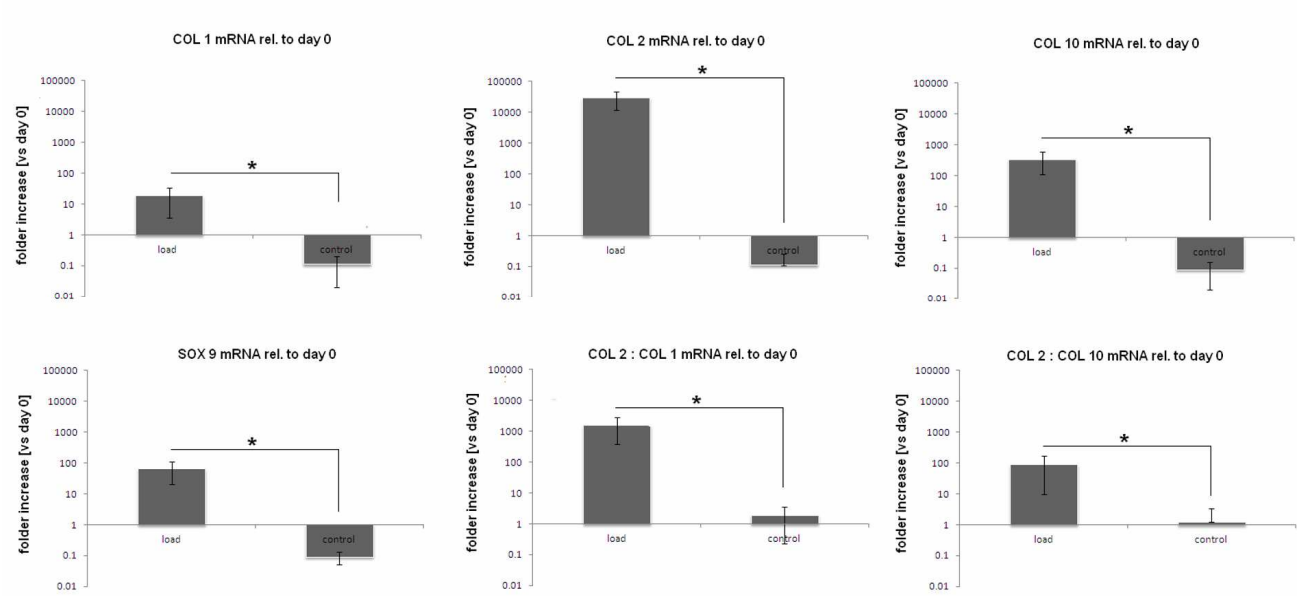

Figure 3. Relative mRNA expression of human mesenchymal stem cells after 21 days of stimulation. Loaded samples showed a clear over-expression of chondrogenic markers collagen 2 (COL 2), collagen 10 (COL 10). Particular, the COL 2 : COL 1 ratio was significant increased by the mechanical load, confirming MSCs chondrogenesis. Bars represent means and standard deviations; all data were normalized to day 0 values.

Collagen 2 (COL 2) and collagen 10 (COL 10) expression are of crucial interest as they are reported in literature as suggestive for cartilage. Considering that the data are normalized to the day 0 expression values, a clear over-expression of COL 2 was noticed after the loading period. The stimulated specimens reported a $2.5x10^4$ folder increase compared to day 0 values, while to controls didn't report same significant results. This represent a very important finding since COL 2 is selective expressed by chondrocytes, suggesting the successful differentiation of MSCs guided by the bioreactor induced forces. Another important result is related to box 9 (SOX 9) expression; it represent and important chondrogenic transcription factor peculiar of cells that are undergoing to the chondrocytes phenotype. As noticed for COL 2, also SOX 9 expression was raised by the mechanical loading; conversely, the control samples expressed very low levels of SOX 9. These two data represent an important evidences that the loaded MSCs were successfully guided towards chondrogenesis. The only gene that was not reported as over-expressed after mechanical loading was collagen 1 (COL 1). This represent an interesting result as COL 1 is strongly related with osteogenesis. Since it was previously demonstrated that is possible to induce osteogenesis by applying compression force alone, what it is possible to assume is that the combination with surface shear is satisfactory to refrain from progressing towards bone. This is not a very surprising finding since it is well established that surface shear forces are strongly involved in the amount and type of matrix synthesis. Therefore, the oscillating movement of the bioreactor was able to successfully

mimic the tensile forces and high hydrostatic pressure that in natural cartilage derive from the synovial fluid water that is retained within the cartilage matrix by the presence of charged proteoglycans. Since the collagen network functions to prevent swelling of the tissue, in the 3D microenvironment of the PU-hydrogel composite, cells were probably induced to produce a strong matrix to face the shear forces generated by the bioreactor. Moreover, the COL 2 : COL 1 ratio value suggested as this matrix was progressively composed mainly by the cartilage specific COL 2. An opened question still remain regarding the data obtained for collagen 10 (COL 10). In fact, COL 10 is representative not only for chondrogenesis but also for hypertrophy. In the literature is not rare to observe enhanced level of hypertrophy related to the use of mechanical forces inductive bioreactors; this fact remain as unclear since one potential reason in vitro MSCs chondrogenesis commonly leads to terminal hypertrophy is because the developing tissue is not stimulated. So, it is possible to suppose that the forces applied in this study were able to induce cells towards chondrogenesis but not enough to completely skip hypertrophy. However, regarding this, the COL 2 : COL 10 ratio value showed how the cells were probably differentiate to a chondrocyte phenotype than to the hypertophic one. In conclusion, PCR analysis proved as the mechanical stimulation was able to induce MSCs chondrogenesis in a MC hydrogel matrix.

2.3.2. Biochemical analysis.

The amount of glycosaminoglycans (GAG) per DNA into the medium was calculated every changes (2 days) while the scaffold amount was calculated at the end of the loading (21 days) (Figure 4 A-C). In general, the observed trend revealed a progressive increase of GAG in the stimulated samples. This data are particularly noticeable looking at the GAG release into the medium (Figure 4 A); the load samples values steadily increased during the 21 days of loading. On the opposite, the GAG accumulated in the medium of the control samples showed only a small increase over the 21 days. These data were also confirmed when the total amount of scaffold GAG accumulation was considered; the difference between loaded and control samples resulted as significantly different ($p<0.05$).

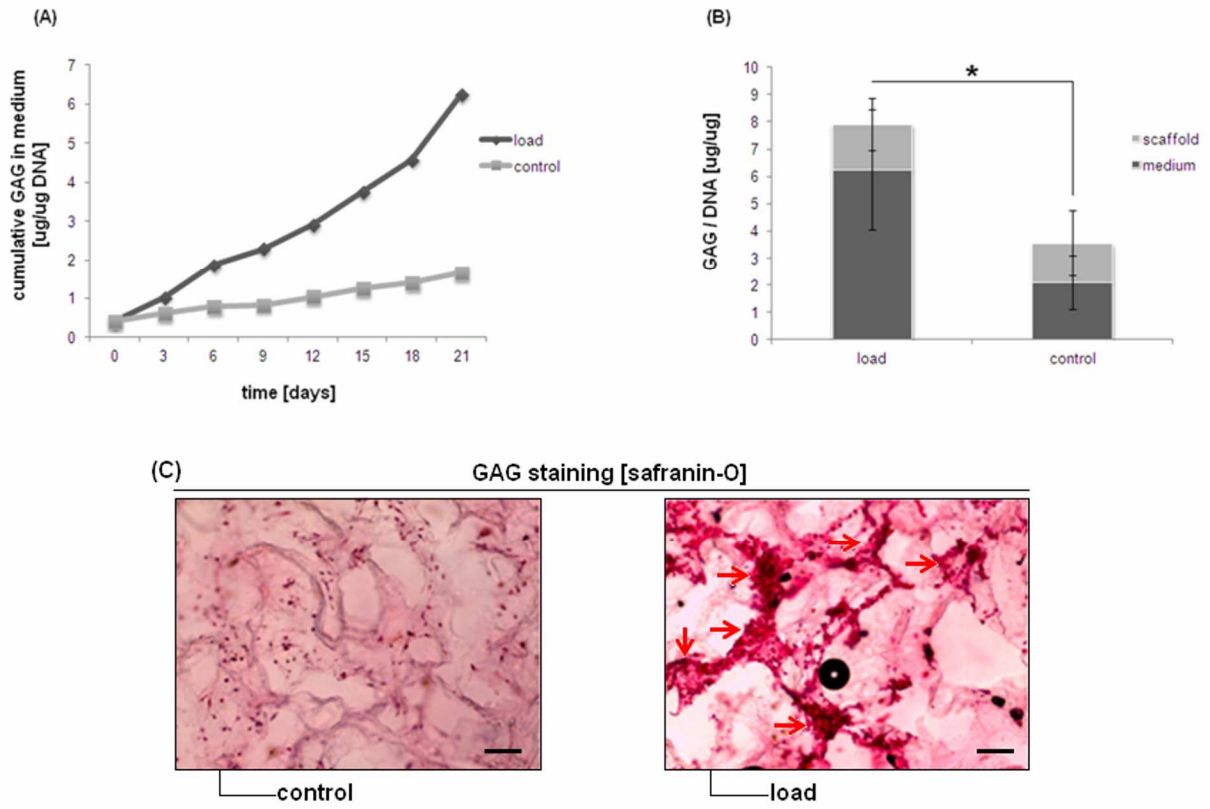

Figure 4 A-C. Accumulated GAG released in the medium over 3 weeks of culture (A); the total amount resulted as increased over the loading period. After 21 days the scaffold GAG amount was calculated and the total amount (medium + scaffold) compared between load and control (B). The total GAG amount was significant different between loaded and control samples ($p<0.05$, indicated by the star). These data were confirmed by the GAG staining using safranin-O (C); the matrix into the loaded samples scaffolds reported a massive amount of GAG while only a small amount was noticed in the control samples. Bar scale=200μm.

From a biochemical point of view, the production of GAG is an important parameter indicating a chondrogenic differentiation. Once MSCs acquire a chondrogenic phenotype, the challenge is to prevent them from becoming hypertrophic. Amongst others, this step is associated with a decrease in GAG secretion. Looking at the time course of GAG secretion in the medium, it was not possible to notice any values decrease indicating a possible hypertrophy appearance. Thus, it is possible to speculate that the loaded cells, even if expressed COL 10, were not undergoing an hypertrophic phenotype. The samples staining with GAG-specific marker safranin-O confirmed the previous results (Figure 4 C); in fact, microscope images showed a massive amount of GAG in the matrix present in the loaded samples pores. On the opposite, the matrix of control samples showed only a small amount of GAG, confirming the crucial role of the mechanical stimulation for chondrogenesis.

2.3.3. Histology.

Loaded and controls samples were investigated towards collagen I and collagen II using immunofluorescence (IF) in order to confirm PCR results. Collagen I staining are reported in Figure 5. PCR analysis revealed a collagen I expression in loaded samples (about 10 folder increase compared to day 0); IF confirmed the presence of collagen I in small amount (lower panel in green) for loaded samples while no signals were detected for the control samples. Thus the IF investigations seems to confirm PCR analysis data.

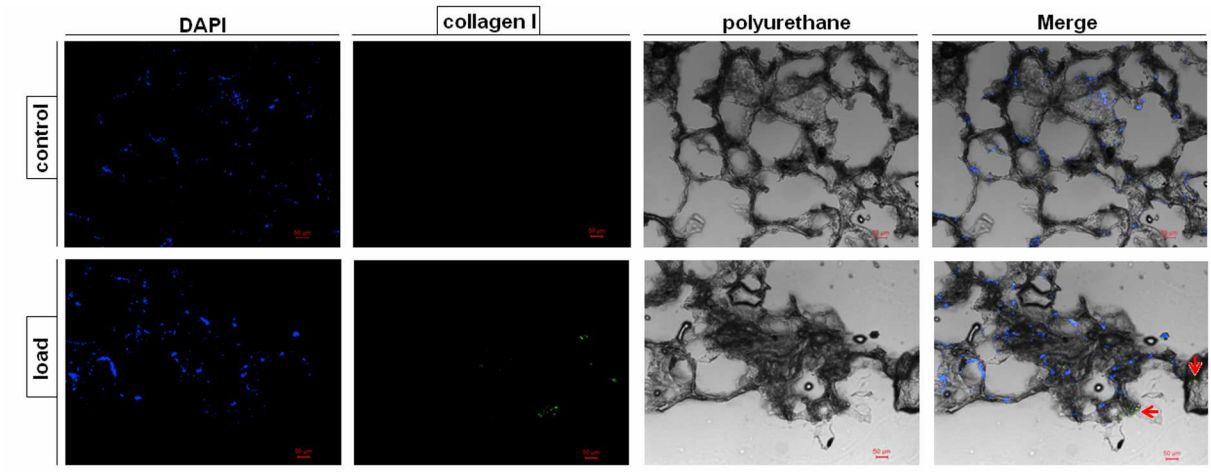

Figure 5. IF collagen I staining. Control samples images did not showed collagen I into the matrix (upper panel), while a small amount was found into the pores containing the matrix of loaded cells (lower panel, green signals).

A very interesting result is related to the collagen II staining, reported in Figure 6. According to PCR analysis, collagen II reported the highest folder increase compared to day 0 of all the investigated genes (more than $2x10^4$ folder increase). The IF staining confirmed the presence of collagen II into the cells matrix of loaded sample (lower panel, in green). The same results was not verified for the control samples that did not showed the presence of collagen II as previously indicated by the PCR analysis. So, also IF staining confirmed PCR analysis data, providing another important proof to the successful bioreactor-guided chondrogenesis.

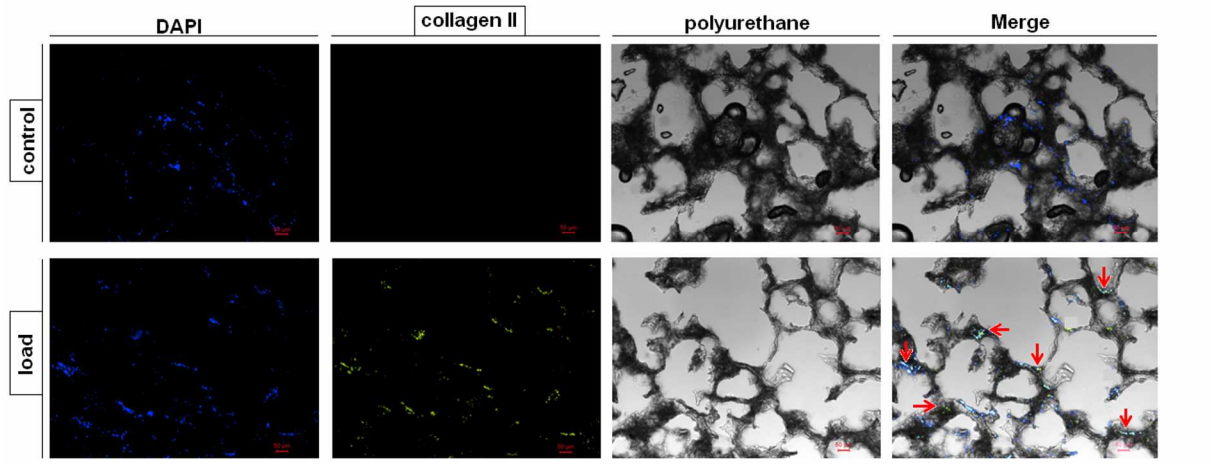

Figure 6. IF collagen II staining. Control samples did not exhibit collagen II (upper panel) while the loaded ones clearly showed the collagen II presence (lower panel, in green).

However, according to the PCR analysis, it was expected to detect a higher amount of collagen II in the scaffolds. A possible explanation of this discordance is that Col 2 up-regulation on the protein level in MSCs is known to be very poor. Even under optimal medium composition, it can take several weeks, and one needs to consider that TGF-β, the most potent factor inducing chondrogenesis, is lacking in the culture medium. Second, as the matrix produced is relatively immature a large proportion is likely to have been released into the medium.

2.4. CONCLUSIONS.

The aim of the work was to evaluate (I) the efficiency of the mechanical induction of chondrogenesis toward MSCs and (II) the suitability of the MC hydrogel as 3D matrix supporting cells development. The data obtained suggested a positive response for both the answers. Cells successfully expressed chondrogenic genes and the GAG quantification confirmed the differentiation route of the MSCs. Histological analysis confirmed the presence of the cells into the PU scaffold pores and the presence of a surrounding matrix of collagen, confirming the suitability of MC-based hydrogel as cells carrier.

Acknowledgments.

A. Cochis would like to thanks Prof. Mauro Alini and Dr. Sibylle Grad of the AO Foundation Research Center of Davos Platz (Switzerland) for all the help during the exchange period and for giving the possibility to use the Muscoloskeletal Regeneration Laboratory bioreactor for the mechanical induction experiments. A special thanks to the European Cooperation in Science and

Technology (COST) Committee for the economical support (grant COST-STSM-MP1005-11184) to A. Cochis.

References.

1. Brittberg M, Lindahl A, Nilsson A, et al. Treatment of deep cartilage defects in the knee with autologous chondrocyte transplantation. N Engl J Med. 1994;331:889-95.
2. Huselstein C, Li Y, He X. Mesenchymal stem cells for cartilage engineering. Biomed Mater Eng. 2012;22:69-80.
3. Diaz-Romero J, Gaillard JP, Grogan SP, et al. Immunophenotypic analysis of human articular chondrocytes: changes in surface markers associated with cell expansion in monolayer culture. J Cell Physiol. 2005;202:731-42.
4. Pittenger MF, Mackay AM, Beck SC, et al. Multilineage potential of adult human mesenchymal stem cells. Science. 1999;284:143-7.
5. Nejadnik H, Hui JH, Feng Choong EP, et al. Autologous bone marrow-derived mesenchymal stem cells versus autologous chondrocyte implantation: an observational cohort study. Am J Sports Med. 2010;38:1110-6.
6. Wakitani S, Mitsuoka T, Nakamura N, et al. Autologous bone marrow stromal cell transplantation for repair of full-thickness articular cartilage defects in human patellae: two case reports. Cell Transplant. 2004;13:595-600.
7. Wakitani S, Nawata M, Tensho K, et al. Repair of articular cartilage defects in the patello-femoral joint with autologous bone marrow mesenchymal cell transplantation: three case reports involving nine defects in five knees. J Tissue Eng Regen Med. 2007;1:74-9.
8. Orozco L, Munar A, Soler R, et al. Treatment of knee osteoarthritis with autologous mesenchymal stem cells: a pilot study. Transplantation. 2013;95:1535-41.
9. Zuk PA, Zhu M, Ashjian P, et al. Human adipose tissue is a source of multipotent stem cells. Mol Biol Cell. 2002;13:4279-95.
10. Hennig T, Lorenz H, Thiel A, et al. Reduced chondrogenic potential of adipose tissue derived stromal cells correlates with an altered TGFbeta receptor and BMP profile and is overcome by BMP-6. J Cell Physiol. 2007;211:682-91.
11. Estes BT, Diekman BO, Gimble JM, et al. Isolation of adipose-derived stem cells and their induction to a chondrogenic phenotype. Nat Protoc. 2010;5:1294-311.
12. Lin Y, Luo E, Chen X, et al. Molecular and cellular characterization during chondrogenic differentiation of adipose tissue-derived stromal cells in vitro and cartilage formation in vivo. J Cell Mol Med. 2005;9:929-39.
13. Zhang HN, Li L, Leng P, et al. Uninduced adipose-derived stem cells repair the defect of full-thickness hyaline cartilage. Chin J Traumatol. 2009;12:92-7.
14. Bahrani H, Razmkhah M, Ashraf MJ, et al. Differentiation of adipose-derived stem cells into ear auricle cartilage in rabbits. J Laryngol Otol. 2012;126:770-4.
15. Elder BD, Athanasiou KA. Hydrostatic pressure in articular cartilage tissue engineering: from chondrocytes to tissue regeneration. Tissue Eng Part B Rev. 2009;15:43–53.
16. Fan JC, Waldman SD. The effect of intermittent static biaxial tensile strains on tissue engineered cartilage. Ann Biomed Eng. 2010;38:1672–1682.
17. von Eisenhart R, Adam C, Steinlechner M, et al. Quantitative determination of joint incongruity and pressure distribution during simulated gait and cartilage thickness in the human hip joint. J Orthop Res. 1999;17:532–539.
18. Huang CY, Hagar KL, Frost LE, et al. Effects of cyclic compressive loading on chondrogenesis of rabbit bone marrow derived mesenchymal stem cells. Stem Cells. 2004;22: 313–323.
19. Huang CY, Reuben PM, Cheung HS. Temporal expression patterns and corresponding protein inductions of early responsive genes in rabbit bone marrow-derived mesenchymal stem cells under cyclic compressive loading. Stem Cells. 2005;23:1113–1121.
20. Mauck RL, Soltz MA, Wang CC, et al. Functional tissue engineering of articular cartilage through dynamic loading of chondrocyte seeded agarose gels. J Biomech Eng. 2000;122:252–260.
21. Heath CA, Magari SR. Mini-review: mechanical factors affecting cartilage regeneration in vitro. Biotechnol Bioeng. 1996;50:430–437.
22. Nicodemus GD, Bryant SJ. The role of hydrogel structure and dynamic loading on chondrocyte gene expression and matrix formation. J Biomech. 2008;41:1528–1536.
23. Villanueva I, Weigel CA, Bryant SJ. Cell-matrix interactions and dynamic mechanical loading influence chondrocyte gene expression and bioactivity in PEG-RGD hydrogels. Acta Biomater. 2009;5:2832–2846.
24. Appelman TP, Mizrahi J, Elisseeff JH, et al. The differential effect of scaffold composition and architecture on chondrocyte response to mechanical stimulation. Biomaterials. 2009;30:518–525.
25. Pelaez D, Huang CY, Cheung HS. Cyclic compression maintains viability and induces chondrogenesis of human mesenchymal stem cells in fibrin gel scaffolds. Stem Cells Dev. 2009;18:93–102.

26. Schatti O, Grad S, Goldhahn J, et al. A combination of shear and dynamic compression leads to mechanically induced chondrogenesis of human mesenchymal cells. Eur Cells and Mat. 2011;22:214-225,.
27. Gorna K, Gogolewski S. Biodegradable polyurethanes for implants. II. *In vitro* degradation and calcification of materials from poly(ε-caprolactone)-poly(ethylene oxide) diols and various chain extenders. J Biomed Mater Res. 2002;60: 592-606.
28. Wimmer MA, Grad S, Kaup T, et al. Tribology approach to the engineering and study of articular cartilage. Tissue Eng. 2004;10: 1436-1445.

Chapter 3.

MC hydrogel as scaffold for the *in vitro* biofabrication of implantable proto-tissues cell sheets.

3.1. INTRODUCTION.

3.1.1. Tissue engineering skills restrictions.

New dares in tissue engineering are directed to the mimicking of the natural environment of a naive tissue. So, the modern strategies for tissue repair and regeneration involve the use of biomimetic materials able to active interacting with the surrounding tissues. These skills are based either on synthetic or natural scaffolds which have been modified at their surface or inside their structure in order to improve their therapeutic efficacy [1, 2]. However, still today the use of scaffolds is often associated with rejection or toxicity problems. Grafts represent a suitable alternative to overcome tissue engineering material problems [3]. However, the availability of tissues and organs is very limited representing a crucial restriction for public health. In fact, autografts are often limited by the poor availability of usable tissues (for example the lack of skin in 3rd degree burns cases) [4]. Allografts are still considered as dangerous for the high rejection risks and also the very limited number of donors [5]. Ideally, high biocompatible materials based on cells cultivated beforehand *in vitro* would be used as alternative. In any case, literature showed a lot of examples demonstrating that cells without support of a suitable scaffolds can just barely form a 3D structured tissue necessary for regenerative purposes [6]. The injection of single cell suspensions has been proposed as a possible strategy to introduce new cells as a source for the input of damaged tissue repair. Even if with this technique some good results has been showed in literature, it is important to notice that in most of the cases injected cells cannot be retained around the target tissue, thus causing difficulties in controlling the location of the injected cells. This could represent a very problematic aspect, since the uncontrolled floating of cells could lead to the unset of conflicts in the non-specific tissues. In particular, the use of stem cells could move to the tumors genesis because of the potency of these cells [6]. Therefore, the improvement of biomaterials-cells composites for regenerative medicine purposes still need further improvements.

3.1.2. Cells Sheet technology.

Common strategies in tissue engineering employing the use of biodegradable scaffolds have so far only shown limited success. To undergo the regeneration of some tissues such as heart, liver or skin, it is necessary to produce complex structures as much cell-dense as possible in order to resemble the native architecture of the natural tissue. Tightly cell-to-cell interaction and cell-to-extracellular matrix (ECM) interaction are crucial for maintaining the tissue and mimic the natural tissue structure. The common in vitro procedures that are necessary for the production of complex

models require the use of proteolytic treatment for the cells cultivation. However, these treatments inevitably cause the degradation of cell surface proteins, which are basic for cell-to-cell and cell-to-ECM interactions (Figure 1 A). Okano et al. have first developed a particular technology known as Cell Sheet in order to overcome these problems [7]. This technique makes it possible to fabricate a sheet composed by high-density cells with their natural extracellular environment (Figure 1 B). Because of its properties and the fact that its fabrication can be subject to automation, Okano et al. showed that cell sheet technology is an ideal approach to biofabrication. Indeed, in biofabrication, when the objective is medical therapy, living cells and bioactive materials are used as building blocks to fabricate advanced biological models on a large scale, and a cell sheet here plays the role of one building block of organ-like structures. The Okano group produced cell sheets using particular polystyrene dishes grafted by a temperature-responsive polymer poly(N-isopropylacrylamide) (PIPAAm) [3]. PIPAAm-coated dishes are temperature-responsive culture dishes where the surface becomes either hydrophilic or hydrophobic in a reversible manner, depending on the temperature. This characteristic has been exploited to detach an intact cell sheet from the culture dishes. The surface of the dishes is relatively hydrophobic, and therefore suitable for cell culture, when the temperature is 37°C or higher. When the temperature is reduced to 32°C or lower, however, the surface of the dish becomes very hydrophilic, and hence confluent sheets of cultured cells can be spontaneously released from the dish surface as described in Figure 1.

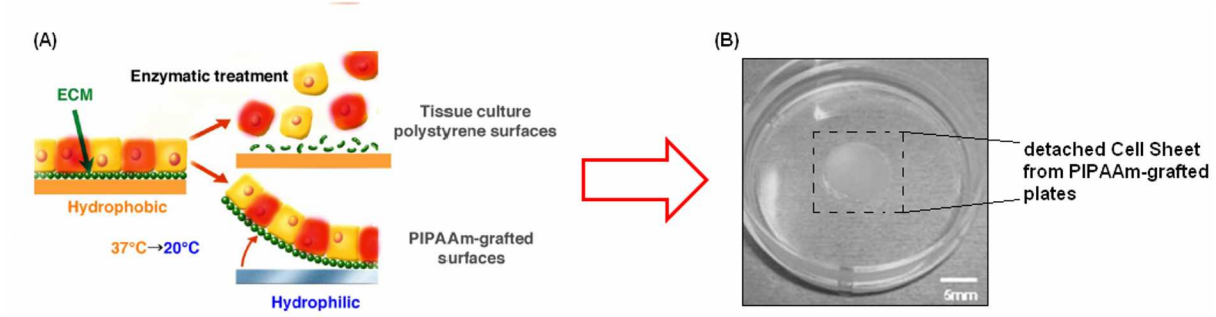

Figure 1 A-B. Schematic representation of the PIPAAm thermo-reversibility mediated cell sheet detachment (A). Avoiding the use of enzymes, it is possible to collect an entire high-density cells monolayer with the natural ECM still present. The final result (B) is an implantable artificial proto-tissue composed by cells tightly interconnected to each other with their natural ECM still present.
(Modified from [6])

The PIPAAm polystyrene plates grafting is based on a very complex process based on an irradiation with an electron beam; therefore, the success of the procedure is vitally linked to the use of polystyrene as cells cultivation substrate [8]. This is a limitation for further procedural

improvements such as the use of bioreactors chambers that need the implication of others materials than polystyrene (for examples those that needs flexibility to respond to a mechanical stimulation). Moreover, the entire production process is very complex and time-consuming, leading to a very high cost of the final product [8]. So, even if PIPAAm grafting represent without any doubt an excellent tool to produce cell sheet of various nature, it is possible to speculate to the possibility of using an alternative polymer for the cell sheets biofabrication.

3.1.3. Clinical evidences.

The cell sheet (CS) technology is relatively recent, but some very encouraging clinical results has already been reported supporting the efficacy of this tool for regenerative purposes. As briefly described in Figure 2, Nishida et al. [9] in 2004 reported the suitability of the CS for cornea regeneration in a patient's damaged eye. Here, As an alternative to corneal epithelial cell sheets, autologous oral mucosal epithelial cell sheets were successfully used without any need for scaffolds or carrier substrates [10]. Patients' own oral mucosal epithelial cells were utilized (Figure 2 A). Epithelial cells, including their stem/progenitor cells, are isolated from a small biopsy and subjected to the fabrication of transplantable epithelial cell sheets (Figure 2 B-C). Clinical results have shown that the corneal surface remains clear with significantly improved visual acuity more than 1 year after the corneal epithelial cell sheet transplantation [11].

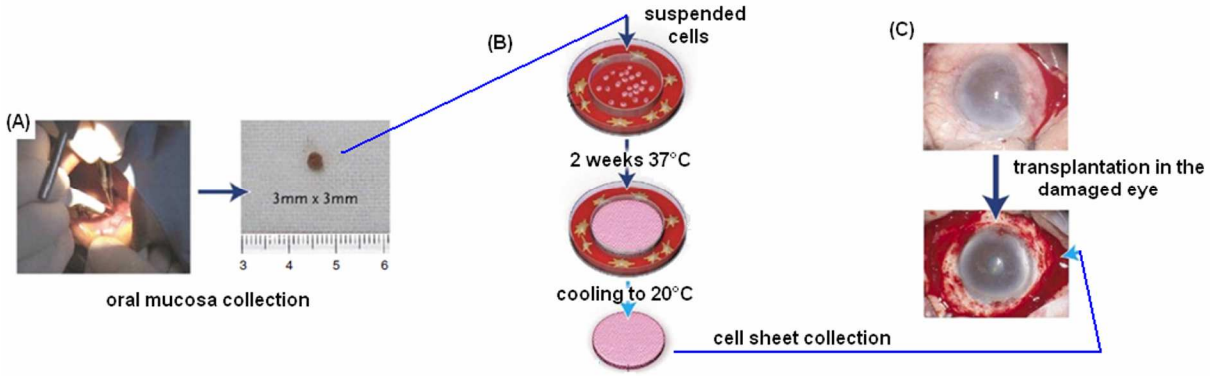

Figure 2 A-C. Schematic representation of the cornea repair described in 2004 by Nishida et al. Patient's own oral mucosa was collected (A) and cells extracted were cultivated onto PIPAAm grafted plate. When a complete monolayer was formed, the entire CS was collected by temperature-depending detachment (B) and implanted into the patient's damaged cornea (C) without the use of sutures.
(Modified from [6])

The cell sheet presents ample features and characteristics which make it an ideal material to use for biofabrication. Indeed, cell sheets can be fabricated from a wide variety of cell types including

periodontal ligament cells [12], esophageal epithelial cells [13], keratinocytes [14], retina pigmented cells [15], corneal epithelial cells [9], oral mucosal epithelial cells [16], cardiac myocytes [17] and others [18, 19, 20, 21]. With cell sheet technology, the use of allogenic feeder cells and fetal bovine serum may be excluded for the preparations [22]. Moreover, cell sheets harvested from temperature-responsive culture surfaces can be directly attached to host tissues without the use of any mediators such as fibrin glue or sutures [23]. Also, upon transplantations, cell sheets attach stably and quickly (5–30 min) to tissue beds due to the presence of the ECM on the basal sheet surface [23]. Furthermore, cell sheets can be layered on top of one another, creating three-dimensional constructs such as thick cardiac muscle.

3.1.4. Aim of the work.

In this third part of the Thesis, the MC-based thermo-reversible hydrogel was investigated as suitable alternative to the PIPAAm grafting for the cell sheet technology. So, the cells adhesion and viability onto hydrogel surface was investigated; afterwards, once cells reach a total confluence forming a continuous monolayer, the hydrogel phase was inverted by cooling down temperature allowing the gel-sol transition. The cell sheet spontaneously detached from the top of the hydrogel; the CS was collected, investigated by immunofluorescence in order to confirm the presence of the interconnected high-density cells. Afterwards, the CS obtained from the hydrogel ability to adhere was in vitro and in vivo investigated, confirming the hypothesis of the intrinsic adhesion ability.

3.2. MATERIALS and METHODS.

3.2.1. Hydrogel preparation.

Methylcellulose (MC, Methocel A4M, with a viscosity of 4.000 mPa*s for a 2% by w/v aqueous solution at 20°C, The Dow Chemical Company, E461) and salts were obtained from Sigma (Sigma Aldrich, St. Louis, MO, USA). Aqueous MC solution was prepared by a dispersion technique as described by Tate et al. [24]. Briefly, 8% w/v MC powder was mixed with a pre-heated (55°C) 0.05M Na_2SO_4 solution in ultrapure MilliQ water (EMD MilliPore Corporation, Billerica, MA, USA) and agitated until all polymer particles were wetted. At 55°C the MC is hydrophobic and remains in suspension. As temperature was lowered to 4°C, the polymer became water soluble, forming a clear solution. Hydrogels were then stored at 4°C overnight to allow complete hydration and heated at 37°C in a 95% humid atmosphere prior to use with cells.

3.2.2. **Mouse fibroblast Cell Sheet (CS) in vitro biofabrication and characterization.**

NIH-3T3 mouse embryo fibroblasts (CRL1658; American Type Culture Collection, Manassas, VA) were used for cell sheet biofabrication protocol standardization. Cells were transduced with third-generation lentivirus, using the pCCLsin.PPT.hPGK.eGFP.pre vector transfer construct as previously described [25]. Cells were cultivated in Dulbecco's modified Eagle's minimal essential medium (DMEM, Sigma-Aldrich, St-Louis, MO, USA) supplemented with 10% foetal bovine serum (FBS, Lonza Group, Basel, CH) and 0.25% penicillin-streptomycin (Gibco, Grand Island, NY, USA) and detached by 0.05% trypsin (Sigma-Aldrich, St-Louis, MO, USA) at 80-90% confluence.

Two hundred microliters of hydrogel were used to coat each wells of a 24 multiwell plate (CellStar, VWR PBI International, Milan, Italy). Plate was heated 2 hours at 37°C in a 95% humidity and coated with 20µl of Type I collagen (BD, 2mg/ml) prior to use with cells. Cells were seeded at high concentration ($1x10^6/cm^2$) onto heated hydrogel surface and cultivated for 48 hours until they reached 100% confluence. Afterwards, 24 wells plate were cooled down to 4°C for 30 minutes to allow hydrogels solid-gel phase transition. Cell sheet spontaneously detached from gel-phase hydrogel without the use of any enzymes and cells sheet were collected by a common 25ml pipette and washed 3 times with phosphate buffered saline (PBS, pH 7.4) before use (Figure 3). Cells adhesion, spread and detachment were visually checked after 8, 12 and 48 hours by fluorescence microscope (Leica DM5500 B, Leica Microsystems, IL, USA). Cells viability was verified by the colorimetric MTT assay; cells cultivated in polystyrene wells coated with collagen I were used as control.

Figure 3. Schematic representation of the cell sheet (CS) detachment from the hydrogel surface. Cells were seeded onto the collagen-coated hydrogel in the sol-phase at 37°C (1) and they were cultivated until a monolayer was formed (2). Afterwards, the system temperature was lowered to 4°C allowing the hydrogel gel-sol phase transition; with liquid hydrogel, CS spontaneously detached as monolayer (3).

3.2.3. Histological analysis.

Detached cell sheets were washed 3 times with PBS, fixed 30 minutes at room temperature with 4% phosphate buffered formaldehyde, embedded in Kilik (Sigma-Aldrich, St.Louis, MO, USA) tissue

freezing compound and stored at -80°C. Samples were cryosectioning at 10μm and slices were seeded 30 minutes onto charged glasses (SuperFrost, Menzel-Glaser, Germany); afterwards samples were stained to visualize F-actins (Molecular Probes Inc, OR, USA) in order to evaluate cell sheet cells distribution, concentration and morphology. Samples were observed with fluorescence microscope (Leica DM5500 B, Leica Microsystems, IL, USA).

3.2.4. *In vitro* Cell Sheet (CS) adhesion.

Detached cell sheets were collected, washed 3 times with PBS and transported to new polystyrene plates previously coated 4 hours with serum. Cell sheet were attached without medium for 5-7 hours; afterwards fresh medium (DMEM 10% FBS) was added and plates were incubated for 48-72 hours at 37°C, 5% CO_2. Cell sheet adhesion was daily checked by optical observation with fluorescence microscope (Leica DM5500 B, Leica Microsystems, IL, USA).

3.2.5. *In vivo* biocompatibility evaluation.

All animals procedures were performed after local ethical committee approval and by following pre-approved surgical procedures. Six-eight weeks old NOD.SCID mice (NOD.CB17-*Prkdc*^{scid}/NCrHsd, Harlan Laboratories) were used for experiments.

NIH 3T3 GFP^{+} cell sheets prepared as previously described were subcutaneous implanted into NOD.SCID mice as described by Obokota et al. [26]. Briefly, a skin pocket was created into the mice dorsal skin with scissors. Cell sheet was introduced in direct contact with natural mice tissues into the skin pocket by using a GoreTex® (Gore and Associates, Arizona, USA) regenerative membrane as scaffold. Afterwards, the pocket was closed with sutures. After 7 days, animals were euthanized and tissues containing cell sheets were collected. Mice implanted with only GoreTex® membrane were used as controls. Experiments were performed in triplicate.

3.2.6. Hystological characterization.

Tissues grafted with cell sheet and control ones were fixed with formalin, embedded in paraffin and sectioned into 10μm slices. Hematoxylin and eosin staining was performed by conventional method as previously described [25]. Samples were analyzed by optical microscope (Leica DM5500 B, Leica Microsystems, IL, USA). Furthermore, tissues were stained with an anti-GFP antibody (anti-GFP, IgG, Alexa Fluor® 488 conjugate, Molecular Probes Inc, OR, USA) to confirm cell sheet adhesion. Samples were blocked with 0.1% BSA in PBS for 90 minutes and reacted with the primary antibody at an appropriate concentration (1:2000) overnight at 4°C. Following three washes

with 0.1% BSA in PBS, they were incubated for 1 h with a 1:1000 dilution of FITC- conjugated anti-rabbit Ig antibody and again washed three times. Immunofluorescence was optically investigated by microscopy (Leica DM5500 B, Leica Microsystems, IL, USA).

3.2.7. Statistical analysis of data.

Statistical analysis was performed using the software package SPSS (Version 18, SPSS Inc, Chicago, IL, USA). Data were analyzed using a general linear model with repeated measures. The significance level was defined at $p< 0.05$. For the post hoc, *p*-values were adjusted according to Bonferroni's method.

3.3. RESULTS and DISCUSSION.

3.3.1. Cells adhesion and viability onto hydrogel surface.

The thermo-reversibility of the 8% w/v MC 0.05M Na_2SO_4 was successfully verified as reported in Figure 4 A. This particular formulation was selected (as previously described in Chapter 1) because resulted the best one from a mechanical point of view in the sol-gel phase transition at 37°C, that is the ideal temperature for cells cultivation in vitro. The presence of salts (sodium sulphate), increased the stability of the hydrogel in a specific phase (solution or gelation), allowing the transition phase stable at 37°C. Thus, the maneuverability of the hydrogel resulted as very serviceable even after or during the phase transition. Cells survived after seeding onto hydrogel surface. As reported in Figure 4 B, when the viability ratio was evaluated by the MTT assay, cells cultivated onto hydrogel surfaces showed a viability comparable with controls and no statistically significant differences were noticed between the two groups. This represent a very promising data as in the previous chapters the suitability of the hydrogel in cells cultivating was tested with a not direct cytotoxicity assay (chapter 1) and as 3D matrix with cells cultivated in the inside (chapter 2). Here it has been reported the viability of cells cultivated on the surface as a 2D monolayer. However, cells adhesion to the hydrogel surface required the presence of a collagen coating. In fact, onto pure hydrogel surfaces, cells tend to aggregate into spherical clusters (data not shown) instead of adhere as single units. Conversely, when a collagen coating was applied, cells correctly adhered to the surface even if the adhesion time needed was superior to the control requiring about 6-8 hours (Figure 4 C). After the adhesion, a correct morphology and spread was observed after about 12-14 hours (Figure 4 C) while a continuous monolayer was formed after 48 hours (Figure 4 C). This phenomenon could be explained considering the low "strength" of the hydrogel layer that act as surface for cells. By definition, hydrogels never reach a solid phase but only a gel phase that is not

comparable with polystyrene. Moreover, the selected hydrogel was voluntarily not considered as the more firm possible but as the best one allowing the possibility to reverse the phase at 37°C. So, it is possible to suppose that even if cells are able to adhere to the nude hydrogel, they need a "guide" to correctly spread as single ones; collagen probably act as guide. The final results are very interesting since it was possible to successfully cultivate cells as monolayer onto hydrogel surface, mimicking the common procedures with polystyrene plates (Figure 4 C).

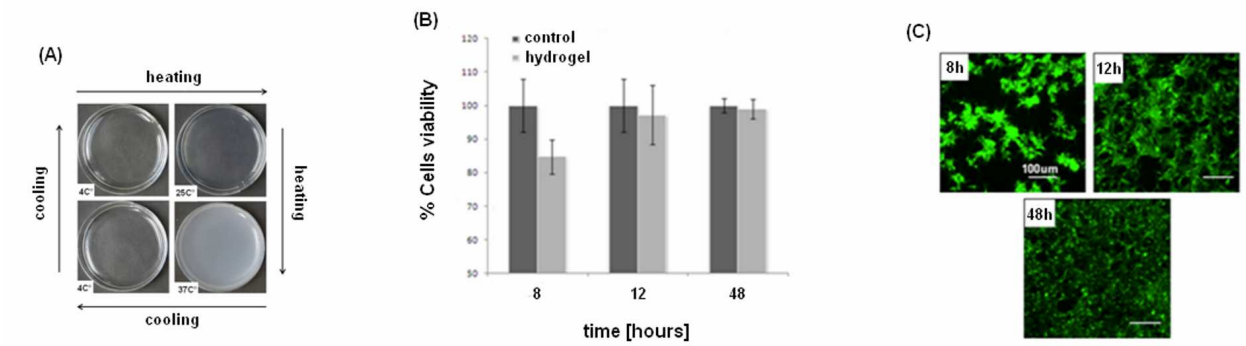

Figure 4 A-C. Hydrogel sol-gel phase transition resulted as reversible since it was possible to invert the phases by modulating the system temperature (A). Cells cultivated onto gel-phase hydrogels reported a viability compared with control at all the time-points and no statistical significant differences were noticed between the control and hydrogel groups (B, bars represent means and standard deviations). Microscope observation (C) revealed that cells correctly adhered and spread in about 12 hours, while a continuous monolayer was formed after 48 hours.

3.3.2. Cell Sheet (CS) *in vitro* characterization.

Once cells reached a 90-100% confluence onto hydrogel surface, the temperature was lowered at 4°C for 20 minutes in order to allow the gel-sol phase transition. As the temperature decreased, it was possible to observe that the cells monolayer initiated to spontaneously detach from the hydrogel surface (Figure 5 A). It is very important to underline that, in the detaching process, no enzymes (such as trypsin) were used permitting the separation of the entire monolayer (Figure 5 B). Finally, when immunofluorescence analysis with phalloidin (Figure 5 C, red) was applied, it was possible to confirm that the CS was actually formed by a 2D monolayer of fully-interconnected cells.

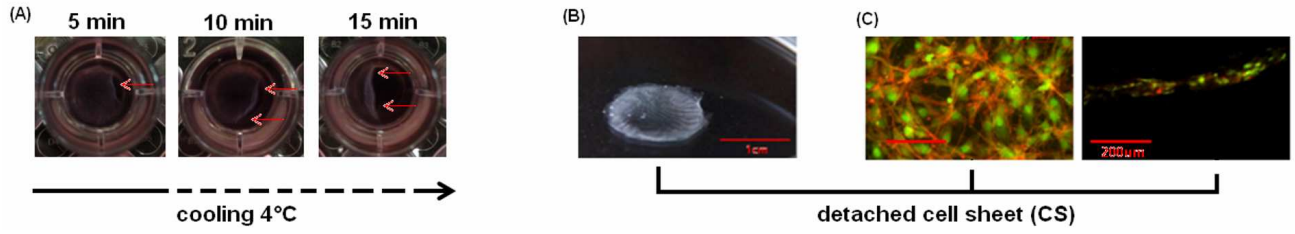

Figure 5 A-C. By lowering the temperature at 4°C for 20 minutes, the cell sheet (CS) spontaneously detached avoiding the use of enzymes (A). As result, it was possible to collect the entire cells monolayer as cell sheet (B); immunofluorescence analysis with phallodin (red) of the detached CS confirmed the 2D monolayer structure of high-density fully interconnected cells (C).

As first proof of the CS ability to adhere to a new surface, it was washed 3 time with PBS and transported with a 25 ml pipette to a new polystyrene plate previously coated 4 hours with serum (Figure 6 A-B). Surprising, the best procedure to support CS adhesion was to allow a first adhesion dry, without the addiction of medium in the new plate. Only some drops of medium were added in order to avoid the CS cells dehydration. By this way, CS attached to the new surface in about 2 hours after that it was possible to add fresh medium without causing CS detachment (Figure 6 B). When the fresh medium was added immediately, the CS was not able to adhere, resulting as floating in it. Also the pre-coating with serum helped the CS adhesion; without the serum pre-coating, the time needed for the adhesion resulted between 6-8 hours. Considering the dry ambient necessary for the adhesion, this represent a very long period for cells without medium. By the serum pre-treatment, the adhesion phase was reduced at about 2 hours, that is an acceptable stage even without medium. The role of serum could be related with the presence of collagen and other protein such as fibronectin that are crucial for cells adhesion. By pre-treating the plate surface with serum, the CS adhesion is probably promoted by these proteins and the time necessary to successfully complete the transplantation is lowered. However, the adhesion ability of the CS is a very interesting point. In fact, a in ideal clinical application of the CS is to implant them directly into the damaged tissue in order to promote and facilitate it repair. Avoiding the use of enzymes such as trypsin in the in vitro procedures, allow to collect a cells monolayer with the natural extracellular matrix (ECM) still present. This represent a crucial aspect for the implant success because the ECM play the fundamental role of connection between the CS and the naïve tissue. These preliminary in vitro results suggested that the CS is able to adhere to a new surface but that the process is speeded by the presence of adhesion proteins; afterwards, after about 12-48 hours, new cells coming from the CS were observed colonizing the free space of the new surface. This is a very promising result about the ability of the CS to induce the regeneration of a damaged tissue since it is the CS itself a first source of cells. Moreover, this re-colonization is supposed to promote the natural regeneration of the naïve tissue.

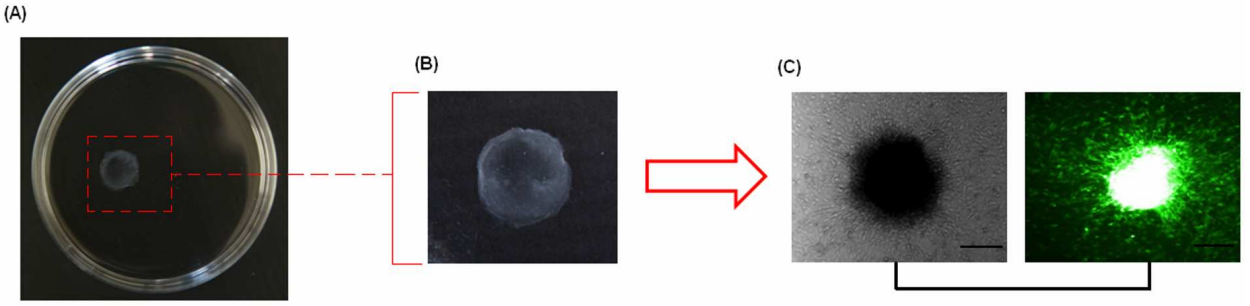

Figure 6 A-C. In vitro transplantation of the detached Cell Sheet (CS). After washing 3 time with PBS (A), the detached CS was plated dry into a new polystyrene plate previously coated with serum (B). The raise of new cells coming from the CS was visually investigated by microscope (C, representative for 48 hours after CS adhesion. Bar scale=200μm).

3.3.3. Cell Sheet (CS) *in vivo* implant.

The CS ability to successfully adhere to a naïve tissue was *in vivo* evaluated. Results are summarized in Figure 7. The CSs were implanted into immune-compromised mice (SCID) because it was possible to speculate the insurgence of immunological reaction for the presence of the GFP. After 1 and 2 weeks, the regions implanted with the CSs were first investigated by Hematoxylin/Eosin staining; at 1 week, it was already possible to notice the presence of a high-density cells monolayer in the correspondence of the CS implant site (Figure 7 B). This layer resulted as different from the naïve tissue because of the very high density of cells (nuclei in violet) tightly interconnected to each others that are characteristics of the CS. Supporting this hypothesis, when the control samples implanted with only Gore-Tex membranes, it was not possible to detect the same cells layer; only the naïve tissue was stained with some debris of the Gore-Tex membrane. As further confirmation of the cells layer-CS correspondence, the same sections were stained by an anti-GFP antibody since the cells used for the experiments expressed the green fluorescent protein. Results confirmed that the cells layer stained with H/E was actually the CS as the cells were positive for the GFP (Figure 7 C). On the opposite, in the control sections, no green signals were detected.

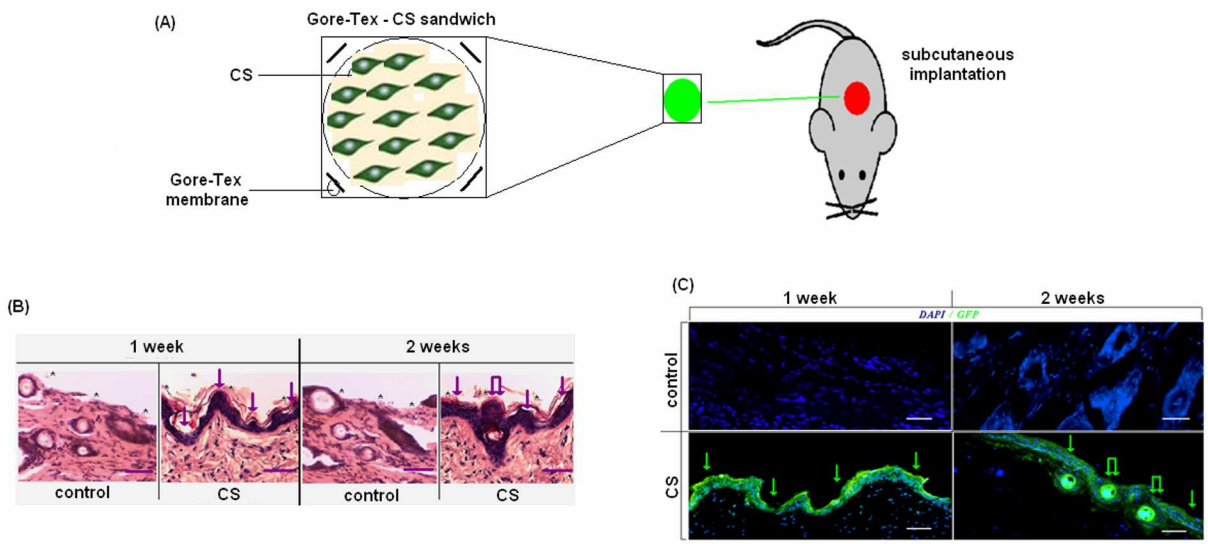

Figure 7 A-C. In vivo evaluation of the CS adhesion to a naive tissue. Gore-Tex-CS sandwiches were subcutaneous implanted into recipient mice (A) and the tissues were collected after 1 and 2 weeks. As first analysis H/E staining revealed the presence of a high-density cells layer attached to the tissue below (B); this result was evident after 1 week while after 2 weeks new vessels were noticed in the correspondence of the CS implant (B, right panel). The presence of the CS was further confirmed by immunofluorescence staining (C); as the CS was composed by GFP^+ cells, a clear green signal was detected in the correspondence of the cells forming the layer previously detected with H/E. Bar scale=200µm.

Another very important finding is related to the presence of vessels that seems to be already connected to the CS implanted. Even if this data must be confirmed by more specific staining, it is possible to suppose that by the H/E staining. If confirmed, this finding could represent a crucial proof for the suitability of the CS in a clinical use. In fact, neo-vascularization represent probably one of the most important step for a positive implantation. The presence of vessels connecting the CS with the naïve tissue represent a very encouraging proof of the CS ability to adhere to the naïve tissue.

When the CSs were implanted, no sutures were used. Therefore, the adhesion of the CSs to the naïve tissue is to refer only the intrinsic characteristics of the CSs. From this point of view, the initial hypothesis that the natural extracellular matrix was still present after the detachment via hydrogel inversion phase seems to be confirmed. In fact, as discussed above, the ECM represent the natural mean for cells adhesion. The H/E staining results underlined as the CSs were perfectly adherent to the naïve tissue with no breaking points. The avoiding of sutures of other connective substance (such as fibrin glue) suggested that the optimal CSs adhesion is to refer without any doubt to the natural ECM. This finding is very important thinking about the suitability of the CSs also for those tissues where is not possible or is very dangerous to apply sutures such as the heart.

Thanks to their ability to adhere by the ECM, the use of CSs for those tissues appear as a promising hypothesis even if the regenerative potential of the tissue-specific CSs must be still confirmed.

3.4. CONCLUSIONS.

In this third part of the Thesis, it was shown the suitability of the MC hydrogel to act as a scaffold for the biofabrication of cell sheets. The cells were able to successfully form a continuous monolayer that was collected entire with the natural ECM still present by exploiting the hydrogel phase inversion. This particular technique is a very promising skill in the tissue engineering field. In fact the CSs are able to adhere to the natural thanks to their natural ECM avoiding the use of sutures. Furthermore, the implanted CSs showed a very promising ability to integrate with the naïve tissue as new vessels were observed towards the implanted regions. Thus, the CSs skill represent an encouraging tool for a future clinical application.

Acknowledgments.

A. Cochis would like to thanks Dr. Andrea Carletta and Dr. Enrico Catalano for the excellent assistant for the *in vitro* cell sheet characterization. Thanks to Dr. Elena Varoni and Dr. Simone Merlin for the help for the *in vivo* surgical procedures. Thanks to Prof. Antonia Follenzi for providing SCID mice and GFP^+ mouse fibroblasts.

References.

1. Hubbell JA. Bioactive biomaterials. Curr Opin Biotechnol.1999;10:123–9.
2. Sakiyama-Elbert SE, Hubbell JA. Design of novel biomaterials. Annu Rev Mater Res. 2001;31:183–201.
3. Wolfe RA, Roi LD, Flora JD, et al. Mortality differences and speed of wound closure among specialized burn care facilities. JAMA. 1983;250:763–6.
4. Alonso L, Fuchs E. Stem cells of the skin epithelium. Proc Natl Acad Sci USA. 2003;100:11830–5.
5. Cardinal M, Eisenbud DE, Armostrong DG, et al. Serial surgical debridement: a retrospective study on clinical outcomes in chronic lower extremity wounds. Wound Repair Regen. 2009;17:306–11.
6. Hannachi IE, Yamato M and Okano T. Cell sheet technology and cell patterning for biofabrication. Biofabrication. 2009;1:1-13.
7. Okano T, Yamada N, Okuhara M, et al. Mechanism of cell detachment from temperature-modulated, hydrophilic-hydrophobic polymer surfaces Biomaterials. 1995;16:297–303.
8. Kim YS, Lim JY, Donahue HJ, et al. Thermoresponsive terpolymeric films applicable for osteoblastic cell growth and noninvasive cell sheet harvesting. Tissue Eng. 2005;11:30-40.
9. Nishida K, Yamato M, Hayashida M, et al. Functional bioengineered corneal epithelial sheet grafts from corneal stem cells expanded ex vivo on a temperature-responsive cell culture surface. Transplantation. 2004;77:379–85.
10. Hayashida Y, Nishida K, Yamato M, et al. Ocular surface reconstruction using autologous rabbit oral mucosal epithelial sheets fabricated ex vivo on a temperature responsive culture surface. Invest Ophthalmol Vis Sci. 2005;46:1632–9.
11. Hayashida Y, Nishida K, Yamato M, et al. Transplantation of tissue-engineered epithelial cell sheets after excimer laser photoablation reduces postoperative corneal haze Invest. Ophthalmol Vis Sci. 2006;47:552–7.

12. Iwata T, Yamato M, Tsuchioka H, et al. Periodontal regeneration with multi-layered periodontal ligament-derived cell sheets in a canine model. Biomaterials. 2009;30:2716–23.
13. Ohki T, Yamato M, Murakami D, et al. Treatment of oesophageal ulcerations using endoscopic transplantation of tissue-engineered autologous oral mucosal epithelial cell sheets in a canine model. Gut. 2006;55:1704–10.
14. Yamato M, Utsumi M, Kushida A, et al. Thermo-responsive culture dishes allow the intact harvest of multilayered keratinocyte sheets without dispase by reducing temperature. Tissue Eng. 2001;17:473–80.
15. von Recum H, Kikuchi A, Okuhara M, et al. Retinal pigmented epithelium cultures on thermally responsive polymer porous substrates. J Biomater Sci Polym. 1998;9:1241–53.
16. Nishida K, Yamamto M, Hayashida Y, et al. Corneal reconstruction with tissue-engineered cell sheets composed of autologous oral mucosal epithelium. N Engl J Med. 2004;351:1187–96.
17. Shimizu T, Sekine H, Yang J, et al. Polysurgery of cell sheet grafts overcomes diffusion limits to produce thick, vascularized myocardial tissues. FASEB J. 2006;20:708–10.
18. Yang J, Yamato M, Shimizu T, et al. Reconstruction of functional tissues with cell sheet engineering. Biomaterials. 2007;28:5033–43.
19. Yang J, Yamato M, Nishida K, et al. Cell delivery in regenerative medicine: the cell sheet engineering approach. J. Control Release. 2006;116:193–203.
20. Yamato M, Sekine H, Yang J, et al. Cell sheet engineering for regenerative medicine: from the viewpoint of inflammation Inflamm Regen. 2007;27:156–64.
21. Yang J, Yamato M, Nishida K, et al. Corneal epithelial stem cell delivery using cell sheet engineering: not lost in transplantation. J Drug Target. 2006;14:471–82.
22. Murakami D, Yamato M, Nishida K, et al. The effect of micropores in the surface of temperature-responsive culture inserts on the fabrication of transplantable canine oral mucosal epithelial cell sheets. Biomaterials. 2006;27:5518–23.
23. Kushida A, Yamato M, Konno C, et al. Decrease in culture temperature releases monolayer endothelial cell sheets together with deposited fibronectin matrix from temperature-responsive culture surfaces. J Biomed Mater Res. 1999;45:355–62.
24. Tate MC, Shear DA, Hoffman SW, et al. Biocompatibility of methylcellulose-based constructs designed for intracerebral gelation following experimental traumatic brain injury. Biomaterials. 2001;22:1113-23.
25. Follenzi A, Ailles LE, Bakovic S, et al. Gene transfer by lentiviral vectors is limited by nuclear translocation and rescued by HIV 1 pool sequences. Nat Genet. 2000;25:217-22.
26. Obokota H, Yamato M, Tsuneda S, et al. Reproducible subcutaneous transplantation of cell sheets into recipient mice. Nat Protoc. 2011;6:1053-9.

Chapter 4.

MC hydrogel-derived cell sheets (CS) for skin regeneration.

In collaboration with the University of Trieste.

Department of Life Science

4.1. INTRODUCTION.

4.1.1. Skin self-renewal limitations.

Numerous factors, of both genetic and traumatic origin, can cause severe skin injuries. Normally, epithelia are able to promote a self-renewal process, which begins with deposition of new provisional tissue matrix by fibroblasts, followed by inflammation, re-epithelization by keratinocytes, and wound revascularization, and concluded by definitive matrix deposition and contraction [1] (Figure 1 A-B). Recently, Mascre´ et al. [2] provided a detailed description of two cell populations in mouse epidermis, identified by specific markers (K14 and Involucrin), that differ in gene expression profile and proliferative and tissue-repair capacity. This finding confirms the concept that epidermis contains long-lived quiescent stem cells as well as committed progenitors in order to self-promote a general strategy for tissue renewal [3]. So, non-severe superficial wounds can be resolved by the skin's self-healing ability by promoting keratinocyte migration toward damaged

regions [4]. However, in deep injuries, a negative regulation of the wound-healing cascade may occur, leading to formation of chronic wounds [5]. In these kind of lesions, re-epithelization can only occur from the wound margins; thus, to prevent extensive scar formation and reduce skin blemishes, skin grafting is necessary [6].

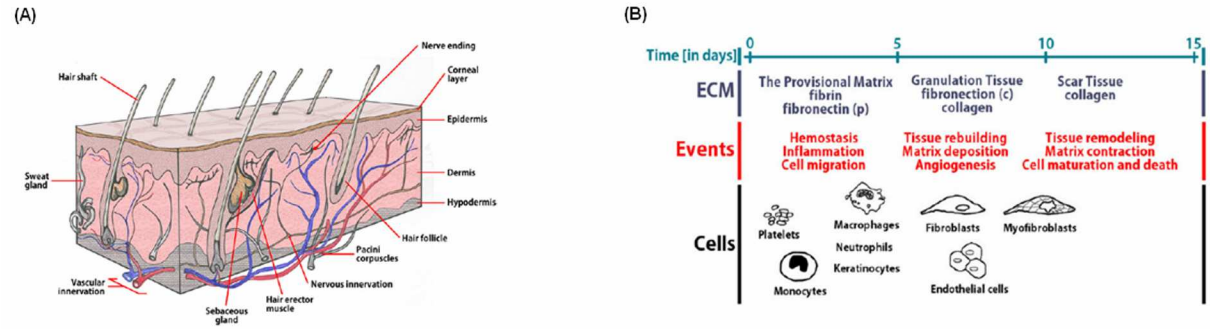

Figure 1 A-B. The normal skin composition (A) and the cascade events of the self repair procedure (B). (modified from [11])

The first surgical step in treating severe skin wounds is the early excision of damaged skin to avoid infections, acute inflammatory response, and marked scar formation [7]. Most frequently, the following step includes autologous skin graft (autograft). This procedure is normally performed with a dermatome, which cuts thin slices of the epidermis and initial part of the dermis; this is a fast and permanent wound-closure method [8]. Nevertheless, whereas this method is effective, it is

limited by the available surface area of unaffected skin and creates some degree of additional injury [1]. Non-autologous skin grafting (allograft) in some situations represents a suitable alternative to autograft. In this case, implantable skin is collected from cadavers. However, allografting leads to a significant number of problems, such as viral transmission (e.g., hepatitis B and C or HIV) and immunogenic rejection [9]. Moreover, commercial distribution of tissue for allografting is provided by a small number of European skin banks, and availability is insufficient to meet the current demand. In most severe cases of burns, one effective solution to avoid patient death can be represented by the implantation of tissue-engineered skin substitutes. Thanks to the use of these engineered substitutes, patients with involvement of a large area of the body have now a better chance of survival [10, 11].

4.1.2. Tissue-engineered skin substitutes.

Tissue-engineered skin substitutes represent an efficient way of meeting the deficiency in donor-skin-graft supplies. They are able to protect damaged regions from fluid loss and contamination and promote release of cytokines and growth factors at the wound site, accelerating the wound-healing processes [12]. They also act as a temporary protective cover of the wound bed during healing. Several commercially available models of engineered skin substitutes have now been developed, which apply different techniques and use different cell sources. Celaderm™ (Advanced BioHealing, New York, NY, USA) is representative of this model, and its efficacy has been validated in clinical trials for treating venous leg ulcers [13]. Alloderm® (LifeCell, New York, NY, USA) is a commercially available de-cellularized tissue-engineered skin substitute consisting of a cell-free matrix permanently incorporated into the wound bed [14]. A further example, represented by engineered skin substitutes and created by the combination of cells and biomaterials, is Dermagraft® (Smith and Nephew, London, UK), which comprises human foreskin fibroblasts cultured in a biologic polyglactin scaffold. This system provides support for extracellular matrix, growth factors, and cytokines released into the wound bed, facilitating the healing process and involving quorum sensing, extracellular matrix formation, paracrine interactions, angiogenesis, immune system interaction, and neutrophil chemoattraction and activation [15]. Another model is a collagen-based, full-thickness, cultured skin substitute [16], which comprises fibroblasts seeded into a bovine collagen type I matrix (dermal side), and keratinocytes cultured at the air–liquid interface (epidermal side) [17]. These products are available commercially as OrCel® (Fortificell Bioscience, New York, USA). All these systems represent very promising tools to face severe skin lesions; however, some questions still remain opened. A very crucial one is related to substitutes

vascularization; in fact, nowadays no models are available presenting vessels before implantation. Furthermore, also the post-implantation neo-vascularization lack has been reported as a common trouble related to skin substitutes [18]. Rejection is another open questions; most of these substitutes are composed by artificial polymers not always able to perfectly integrate into host body [19]. Moreover, when polymers are enriched with cells, these are often non-self leading to inflammation reactions processes. In this context, the cell sheet (CS) technology represent an interesting alternative. In fact, it allow to implant a layer of cells without the necessity of a polymer as scaffold, skipping all the risks related to the polymer biocompatibility. The cell source could be the patient itself, allowing the possibility to implant self-cells. Moreover, it has been previously showed (Chapter 3) as the CS have the ability to spontaneously adhere to the naïve tissue without the use of sutures by the cells natural ECM. The *in vivo* model previously detailed in the results session of the Chapter 3 suggested that the CS were vascularized after a short period, giving encouraging promises for the successful ability to adhere to damaged skin leading to the regeneration process.

4.1.3. Elastin-based biopolymers for biomedical applications.

Bio-mimicry, the concept of taking inspiration from nature is perhaps among the most appealing strategies to create customized biomaterials with finely tuned peculiar features. Elastomeric proteins are among the components that received considerable attention. Elastin, one of the components of the extracellular matrix, possesses rubber-like elasticity undergoing deformation without rupture and provides an important model for biomaterials design. Another peculiar extensively studied characteristic of elastomeric proteins is coacervation. Under appropriate conditions of concentration, ionic strength and increasing temperature, the protein is known to separate from solution as a second phase. It has been shown that this behavior is mainly due to the presence of the hydrophobic (VPGXG) pentapeptide, typical of the mammalian protein [20]. In the human protein, the most structurally regular sequence is represented by the repetition of the (VAPGVG) hexapeptidic motif. It has been shown that the VAPGVG motif is biologically functional [20].

By a molecular biology approach, a regularly repeated domain from human tropoelastin was chosen as a basic modulus to obtain the Human Elastin-Like Polypeptides (HELPs). These artificial proteins can be employed in the production of innovative micro- and nano-structured biomaterials with a huge potential for employment in the biotechnological and biomedical fields [21].

4.1.4. Aim of the work.

In this part of the Thesis, the CS technology was applied for the skin regeneration purpose. Considering the 3rd degree burn as clinical problem, the CS were realized with human primary fibroblasts extracted from the gingival tissue (HGF) considering that patients normally does not present enough or potentially regenerative skin regions. In order to improve the CS-skin model, a layer of HELPs has been used as feeder for HGF cultivation on the MC-hydrogel. The purpose was to improve the mechanical and biochemical features of the implantable CS. The HELP-HGF CS were collected and used for skin regeneration in a 3rd degree model in mice consisting in the skin complete excision. The natural regeneration was considered as control. The skin-CS implant give very promising results as the skin defect was successfully repaired in about 1 week, while the natural process needed at least 2 weeks.

4.2. MATERIALS and METHODS.

4.2.1. Primary Human Gingival Fibroblast extraction and cultivation.

Primary human gingival fibroblasts (HGF) were isolated from a fresh gingival biopsy collected from tissue excided from healthy teeth obtained from orthodontic procedures. The entire tissue was minced with a surgical blade and digested 45 minutes at 37°C with a solution of 1% Type I collagenase I, 0.1% dispase I (Worthington) and 25% trypsin (Sigma) in a serum free minimal essential medium alpha modification (α-MEM, Sigma). Afterwards, digested solution was 0.45μm filtered in order to remove undigested debris and centrifuged 10 minutes at 800 rpm. The pellet was then resuspended in α-MEM supplemented with 10% foetal bovine serum (FBS, Sigma), 1% antibiotics/antimycotics (penicillin/streptomycin/gentamycin, Anti-Anti, Sigma) and plated into new polystyrene Petri plates containing fresh medium. Cells were grown up to a maximum of about 80% confluence and detached with trypsin/EDTA before use; cells from passage 1 to 3 were used for experiments.

4.2.2. Methylcellulose hydrogel– Human Recombinant Elastin composite preparation.

Methylcelulose (MC) derived thermo-reversible hydrogel was prepared as previously described in Chapter 3, paragraph 3.2.1. Two hundred microliters of liquid hydrogel were spotted into each wells of a 24 multiwell plate that was hydrated O.N. and heated 2 hours at 37°C prior to use. The Human Elastin-Like Polypeptides (HELP) were kindly provided by Prof. Antonella Bandiera; HELP were prepared as described elsewhere [21] and used at a final concentration of 4mg/ml. At this concentration, the sol-gel transition of HELP solution results as no reversible; thus, a continuous

HELP layer was realized onto the hydrogel surface by spotting 50µl of liquid HELP solution. Afterwards, MC-hydrogel-HELP composites were incubated at 37°C 2 hours prior to use with cells to allow the complete HELP layer solidification; to improve cells adhesion, 20µl of type I collagen (BD Bioscience, 2mg/ml) were even used to coat HELP surface (Figure 2 A). Cells (HGF) were seeded at high-density ($3x10^4/cm^2$) onto the MC-hydrogel-HELP surface and cultivated 48 hours at 37°C, 5% CO_2 atmosphere using α-MEM. Cells adhesion and spread were investigated by immunofluorescence staining using phallodin (AbCam, 1:500) to visualize F-actins cytoskeleton structure; images were collected using a fluorescence microscope (Leica DM5500 B, Leica Microsystems, IL, USA). The colorimetric MTT assay (Sigma) was used as described in the previous chapters in order to verify cells viability.

4.2.3. HELP-HGF CS collection and *in vitro* characterization.

Cells were cultivated onto MC-hydrogel-HELP composites for 48 hours, daily checking the cells adhesion, spread and confluence by fluorescence microscope. After 48 hours, HGF formed a continuous monolayer and the cell sheets formed by HELP and HGF (named by now skin-CS for their application) were detached by lowering the system temperature to 4°C for 20 minutes allowing the MC-hydrogel gel-sol phase transition. Skin-CS spontaneously detached from the hydrogel surface as monolayer that were collected, washed 3 times with PBS and used for in vitro characterization. Skin-CS were washed 3 times with PBS, fixed 30 minutes at room temperature with 4% phosphate buffered formaldehyde, embedded in Kilik (Sigma-Aldrich, St.Louis, MO, USA) tissue freezing compound and stored at -80°C. Samples were cryosectioning at 10µm and slices were seeded 30 minutes onto charged glasses (SuperFrost, Menzel-Glaser, Germany); afterwards samples were stained with phalloidin (AbCam, 1:500), type II collagen (AbCam, 1:150) and a HELP-specific primary antibody. Samples were incubated O.N. at 4°C with the primary antibody and then co-stained with the appropriate secondary antibody (1:500). Samples were observed with fluorescence microscope (Leica DM5500 B, Leica Microsystems, IL, USA).

4.2.4. *In vivo* 3rd degree burn treatment using skin-CS.

Skin-CS were *in vivo* tested for their regenerative potency towards damaged skin. All animal procedure was performed after local committee approval and by using pre-approved surgical procedures. A 3rd degree burn skin damage was *in vivo* simulated using nude mice (Hsd:Athymic Nude-*Foxn*^{nu} mice, obtained from Harlan) as described by Ma et al. [22]. Briefly, a 1cm diameter skin excision was create using forceps into the dorsal side (both left and right side) of recipient

mice; the right side excision was filled using the skin-CS as regenerative tool, while the left side was not treated and considered as control for the mice natural regeneration ability. The skin-CS were attached to the skin defects by spotting some drops of fibrin glue (prepared following the manufacturer's instructions (Sigma)) around the excision boundaries. The same procedure was followed for the control excisions. Mice were sacrified after 1, 2 and 3 weeks after implantation; the skin excisions regions were collected, fixed by 24 hours immersion in buffered formalin and stored at -80°C embedded in Kilik (Sigma-Aldrich, St.Louis, MO, USA) tissue freezing compound.

4.2.5. Hystological analysis.

Tissues samples were cryosectioning at 10μm and slices were seeded 30 minutes onto charged glasses (SuperFrost, Menzel-Glaser, Germany); afterwards samples were stained with Hematoxylin and Eosin (H/E) following manufacturer's instructions (Sigma) in order to evaluate the new-formed tissue around the skin excision. Furthermore, slices were incubated with anti-alpha smooth muscle antibody (α-SMA, 1:150, AbCam) and co-stained with the 4',6-diamidino-2-phenylindole (DAPI, Sigma) the in order to study the neovascularisation and co-visualize the cells nuclei.

4.4. RESULTS and DISCUSSION.

4.4.1. MC-hydrogel-HELP composites production.

The Human Elastin-Like Polypeptides (HELP) solution successfully adhered to the methylcellulose-based (MC) hydrogel forming a continuous and homogeneous layer (Figure 2 B). The HELP solution was prepared at a concentrations of 4mg/ml; this high amount was voluntary selected as the HELP solution-gelation phase was not anymore reversible. In fact, HELP polypeptides act in solution as an hydrogel by moving from a liquid solution at 4°C to a solid-gel phase at 37°C. However, HELP hydrogel could not be considered as a smart materials like MC-hydrogel since the use of enzymes is necessary to carry on the phase transition. Thus, temperature is not the only parameter necessary for the transition to the gel phase. Furthermore, a HELP peculiar is that the eventually phase reversion to the liquid phase is inseparable related to the polypeptides concentration; the selected 4mg/ml concentration allow to obtain a very compact layer of elastin which gel phase is not reversible anymore to the liquid phase.

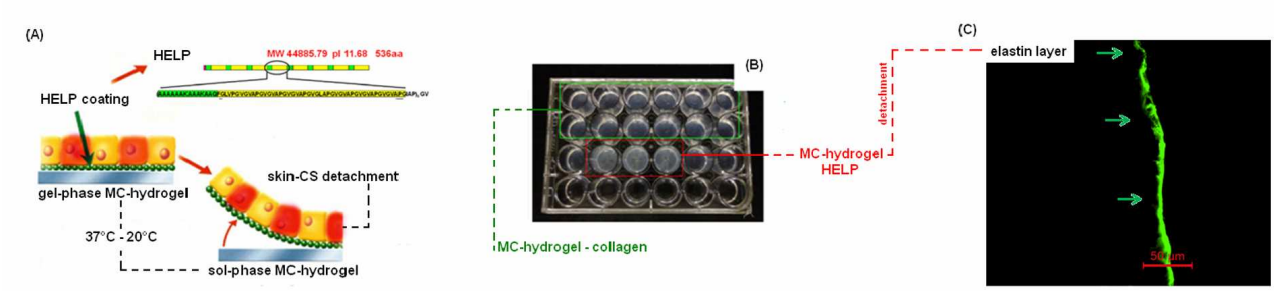

Figure 2 A-C. Representative scheme of the skin-CS biofabrication using the MC-hydrogel as scaffold and the elastin layer as cells support (A). The addiction of the HELP layer has not interposed the hydrogel phase-transition process for the CS production; the composites resulted as stable and comparable with the previous model with collagen alone (B). The HELP layer (cells free) was successfully detached from the hydrogel surface (C).

This step is fundamental for the successful HELP-enriched cell sheet (CS) detachment; in fact, the spontaneous CS detachment is leaded by the temperature decrease that permit the MC-hydrogel phase transition from gel to liquid. If the HELP layer was still sensitive to temperature, this step inevitably damaged the layer that was reported to the liquid phase too. Thanks to the high polypeptides concentration, the HELP layer remained in the gel phase even when the temperature was lowered, allowing the detachment of a continuous layer (Figure 2 C). This layer represent the holding structure for the skin-CS development.

4.4.2. HELP-HGF CS production.

Human gingival primary fibroblasts (HGF) were successfully extracted from fresh tissue isolates; after tissue digestion, single cells suspension attached to plates surface and proliferate (Figure 3 A). Cells seeded onto HELP layer correctly attached to the surface in about 12 hours; afterwards, a cells monolayer was observed after 48 hours of cultivation (Figure 3 B). Cells viability was verified by the MMTT assay: at each time-points, cells viability percentage was comparable with controls and no statistically significant differences were observed between the two groups (Figure 3 C). This findings are encouraging because they are very similar with the data obtained with mouse fibroblasts and described previously in Chapter 3. Therefore, the presence of the HELP layer seems to not interfere with the cells adhesion, spread and viability.

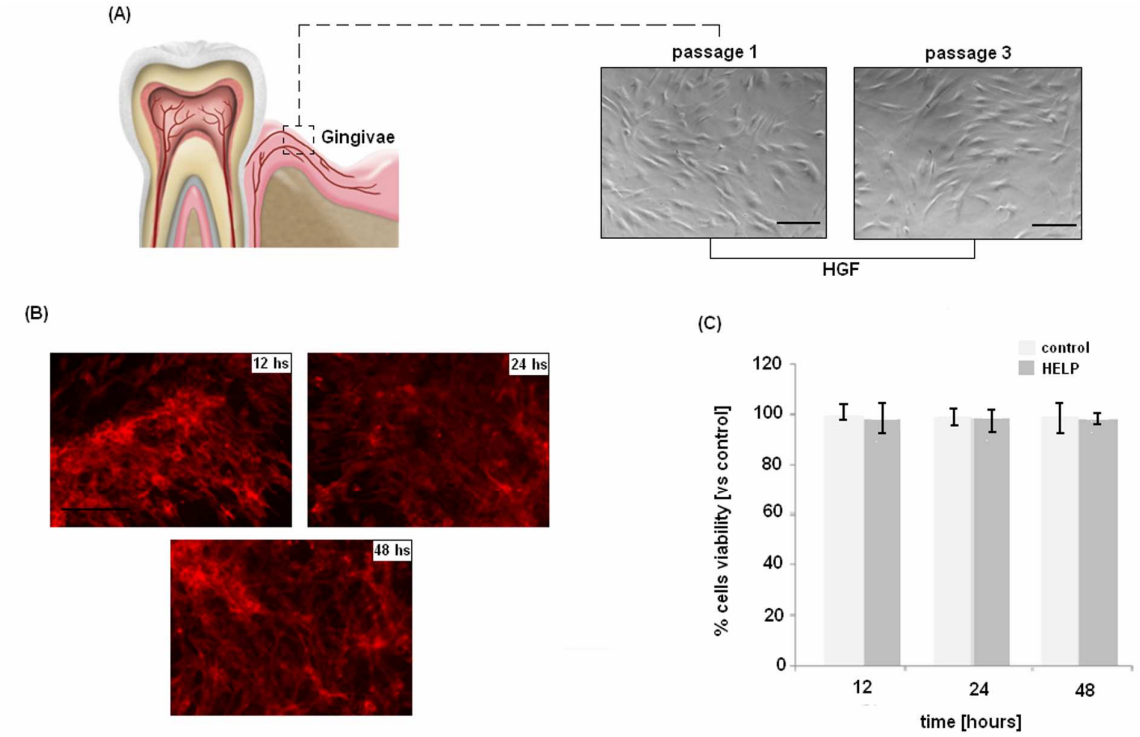

Figure 3 A-C. Human primary fibroblasts were obtained by enzymatic digestion of fresh tissues and used from passage 1 to 3 (A). The cells seeded onto HELP layers adhered to the surface in about 12 hours and a continuous layer was observed after 48 hours by phalloidin staining (B in red). Finally, cells viability onto HELP surface was comparable with controls (C). Bars represent means and standard deviations, bar scale=200μm.

This is an important step in the protocol development. The improvement of the CS tool by the addiction of the HELP layer was aimed to enhance the mechanical properties and the matrix complexity of a model studied for the skin regeneration. In fact, skin represents a stratified complex tissue holding a remarkable flexibility from a mechanical point of view. Thus, the skin-CS present an elastin layer that (I) act as an improvement of the natural cells ECM and (II) confers to the CS a better mechanical ability to fit with natural tissue.

4.4.3. Skin-CS characterization.

Detached skin-CS immunofluorescence staining are reported in Figure 4. The cell sheets are composed by cells tightly connected to each other forming a continuous monolayer as showed by phalloidin stain. Cells morphology resulted as correct confirming the adhesion study results. One of the improvement speculated by the addiction of the elastin layer was related to the enrichment of the natural ECM. Collagen II staining confirmed that the cells forming the detached skin-CS (I) successfully produced and (II) maintained their natural matrix. This finding is very important since a crucial feature of the cell sheet technology is the ability of adhere to a naïve tissue without the use of sutures thanks to the presence of cells ECM that act as “glue”. Cells produced high amount of

collagen as reported in Figure 4, upper panel. By staining the skin-CS sections in the lateral side, it was possible to appreciate the monolayer of cells interconnected and supported by the elastin layer (lower panel). Cells correctly spread onto elastin layer forming a complex composite.

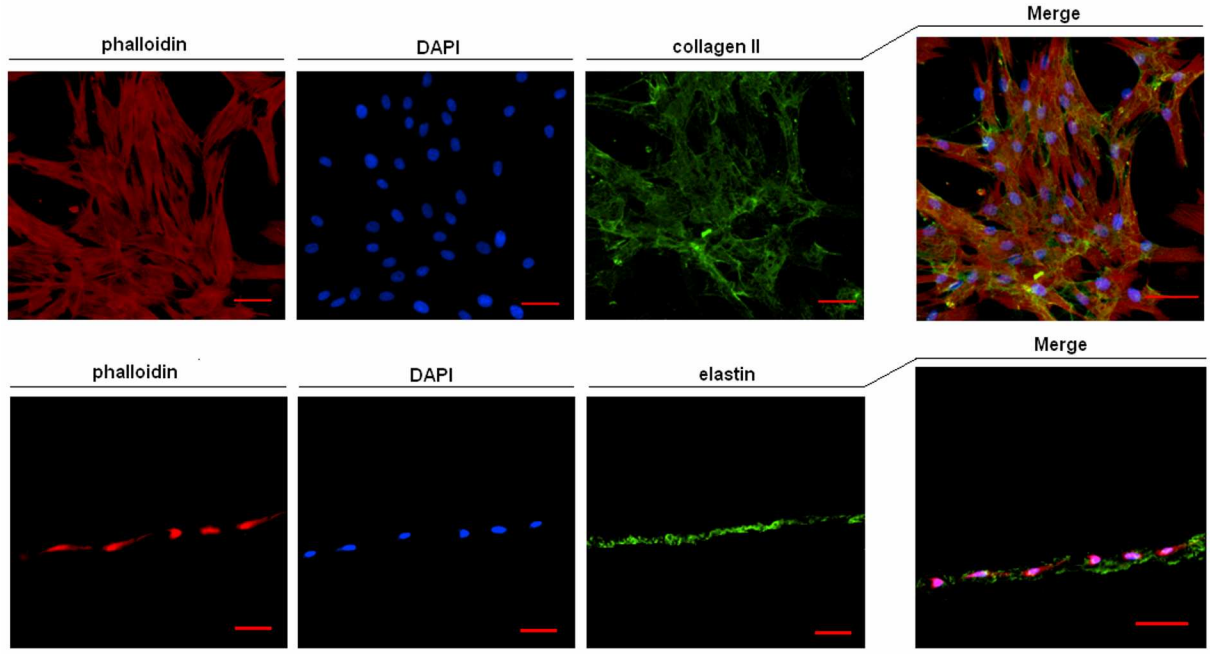

Figure 4. Immunofluorescence staining of detached skin-CS. The cells sheets resulted as formed by high-density cells interconnected to each others; furthermore, cells were able to produce collagen onto the elastin layer (upper panel). By cutting the skin-CS in the lateral side, it was possible to appreciate the cells monolayer interconnected with the elastin layer that act as matrix in addition to the natural collagen (lower panel). Bar scale=50µm.

Thus, it was verified the possibility to prepare a cells-elastin skin-CS. The entire protocol was comparable to the cell sheet production using the MC-hydrogel as scaffold described in Chapter 3 as no significative modifications were applied. This is an important data since it suggests that it is possible to introduce improvements in the cell sheet without compromise the hydrogel thermo-reversibility. So, it will be possible in the future to further improve the technology (for example by trying to orientate the cells). The skin-CS composites reported matrix very interesting features; in fact, the presence of the natural collagen produced by the cells was verified together with the connection with the elastin layer. Therefore, the entire matrix of the skin-CS resulted as very complex allowing to improve the adhesion to natural tissue. The regenerative potency and the ability to support the mechanical stress related with the natural skin will be verified by the *in vivo* test.

4.4.4. Skin-CS regenerative potency *in vivo* evaluation.

The implanted skin-CS were able to adhere to the mice tissue without sutures and to promote skin regeneration in a significative lower time lap compared to the natural process. In vivo assay results are summarized in Figure 5.

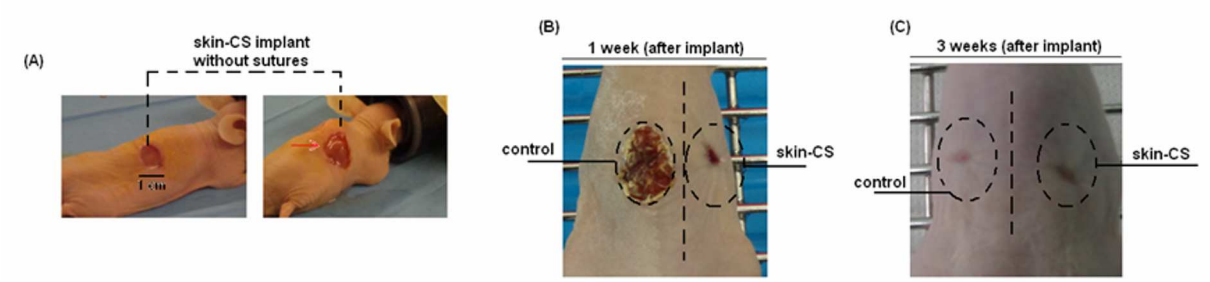

Figure 5 A-C. In vivo 3rd degree burn skin damage repair (A). The skin-CS were attached to the skin defect using fibrin glue (A, right panel); after 1 week the skin-CS implant side showed to be able to promote a faster regeneration (B, right side) compared to the natural tissue regeneration ability (B, left side). After 3 weeks, also the natural repair process regenerated the damaged region (C, left) even if the skin-CS implanted side appeared as more compact (C, right).

After 1 weeks after skin-CS implant, a great difference was noticed compared to the control. In fact, the skin-CS were able to promote a very fast and successful regeneration of the artificial damage (Figure 5 B). On the opposite, the natural repair process did not showed new generated skin. The natural process was comparable with the skin-CS only after 3 weeks (Figure 5 C); however, by handling the skin for the excision after mice sacrifice, it was possible to notice that the CS implanted skin was more dense and thick. The differences between the skin regeneration induced by CS and natural process were very noticeable by hematoxylin/eosin (H/E) staining of the collected tissues and by the neovascularization investigation by immunofluorescence (IF).

In Figure 6 are reported the H/E and IF analysis of the 1 week sections.

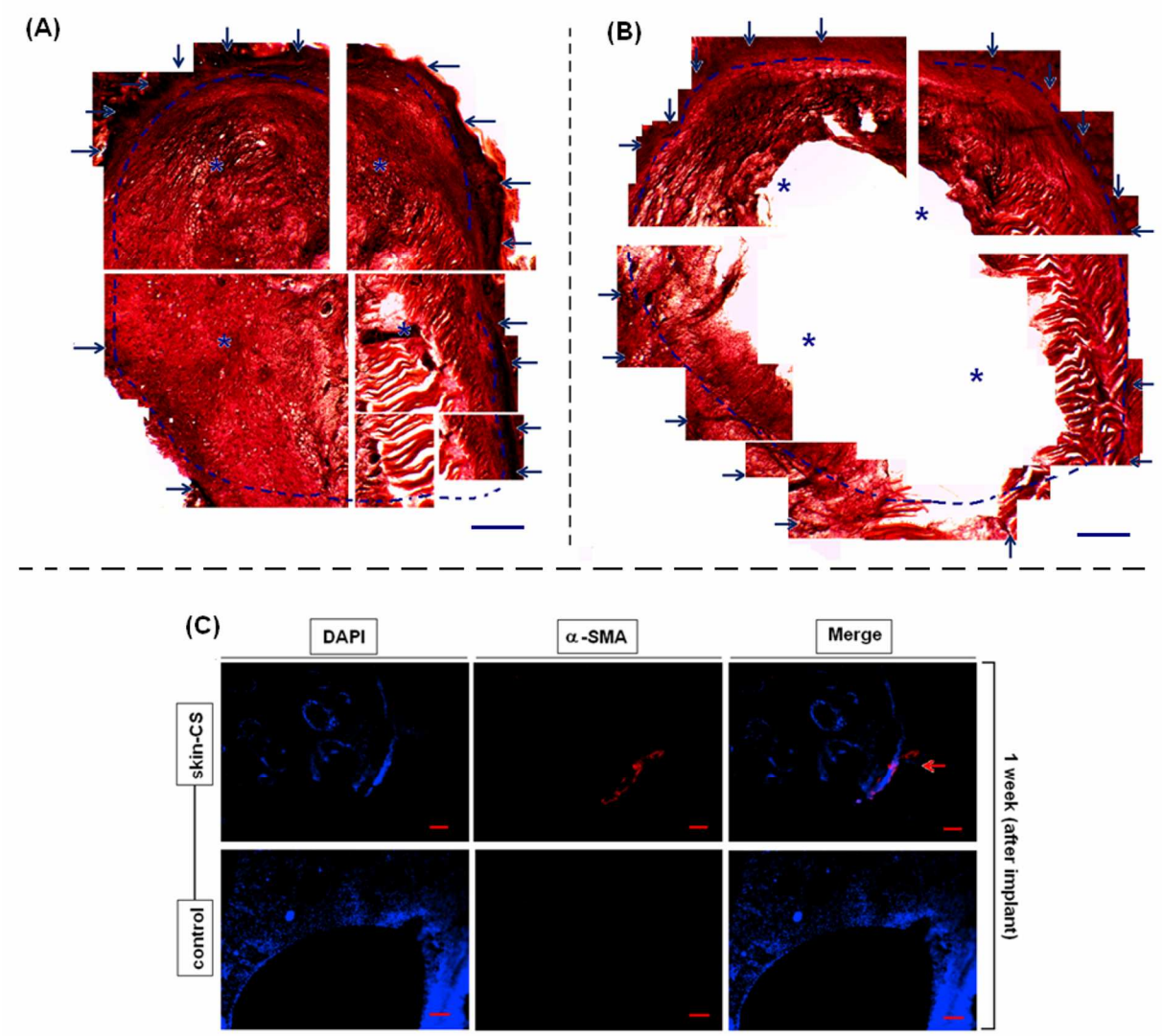

Figure 6 A-C. 1 week implants analysis. H/E analysis of the skin defect regions revealed that the skin-CS was effective in the regenerative process induction (A, stars indicate the new formed tissue, arrows and lines the defect limits) that was not yet started in the natural repair process (B). Furthermore, in the skin-CS implants region, new blood vessels were noticed by staining with a-SMA (C, in red); no vessels were visualized in the controls. Bar scale=200μm.

In Figure 6 A, the skin-CS implanted region is showed. The arrows indicate the limit of the artificial defect created by skin excision, while the stars indicate the new-formed tissue. In the skin-CS implant, the regeneration was clear. New tissue was visualized all around the limits of the excision; moreover, the new-formed tissue appeared as compact and thick with no lack regions. On the opposite (Figure 6 B), the control sections appeared as devoid of tissue in the excision region. This is a very important finding as suggest that the cells layer composing the skin-CS was successfully attached to the naïve tissue undergoing and helping the restoration process. Moreover, the elastin-collagen complex matrix of the skin-CS lead to the formation of a thick and dense layer comparable with the natural tissue. During the first 7 days of implantation, mice were daily checked and no

movements limitation caused by the skin excision were noticed; moreover, none of the mice reported the skin-CS detachment during the test period as confirmation of the optimal adhesion property of the cells elastin-improved ECM. Another important result is related to the presence of blood vessels inside the excision region where the skin-CS were implanted (Figure 6 C); in fact, neovascularization is a crucial step in the regenerative process, as the vessels are the "tools" to include the new-formed tissue into the natural counterpart biochemical signaling. The lack of vessels normally lead to the failure of the implant. Obviously, in the control no vessels were visualized as no tissues was present yet; this data was confirmed by DAPI staining that evidenced the excision region limits (Figure 6 C).

Results after 3 weeks of implant are reported in Figure 7. After 21 days, the skin-CS implanted regions resulted as completely repaired with no lack of tissue in the neo-formed part (Figure 7 B). at this time-point, also the controls showed the presence of new-formed tissue in the excision regions. Thus, also the natural repair process was effective in the skin regeneration. However, the H/E staining revealed that the skin-CS region was composed by a more dense and thick tissue, comparable to the natural one. This is not a surprising data because the regenerative process was found to be effective since the first week, suggesting that the new-formed tissue was undergoing a complete integration in the following two weeks. The better host-guest integration of the skin-CS derived new-formed tissue was confirmed by the neovascularization analysis. The control showed the presence of vessels confirming that the natural process was effective undergoing after 3 weeks; however, the number and complexity of vessels network was superior for the skin-CS regions. This represent a confirmation of the H/E results that lead to suppose that the regenerative process was induced by the presence of the skin-CS faster than the natural process; thus, even if after 3 weeks it was possible to notice for both control and skin-CS a regeneration process, the skin-CS derived new formed tissue was completing the integration process, while the controls were still facing the production of tissue and vessels.

In conclusion, the skin-CS regenerative potency in a 3rd degree burn defect was confirmed. The implant of skin-CS improved the natural ability of the naïve tissue to repair the tissue damage. This is the most important finding thinking of a possible clinical application. In fact, the appliance of skin-CS could be moved in a patient self-process by collecting a small biopsy from the gingival tissue skipping the rejection process. The skin-CS could be applied to the damaged tissue without sutures; the regenerative potency of the skin-CS could help the repair of the injured tissue and, more important, supply to the loss of the regenerative process in the damaged site such as 3rd degree

burns. Thus, even if more evidence are still necessary to validate the clinical use of the skin-CS, this tool represent a very promising technique for skin tissue engineering.

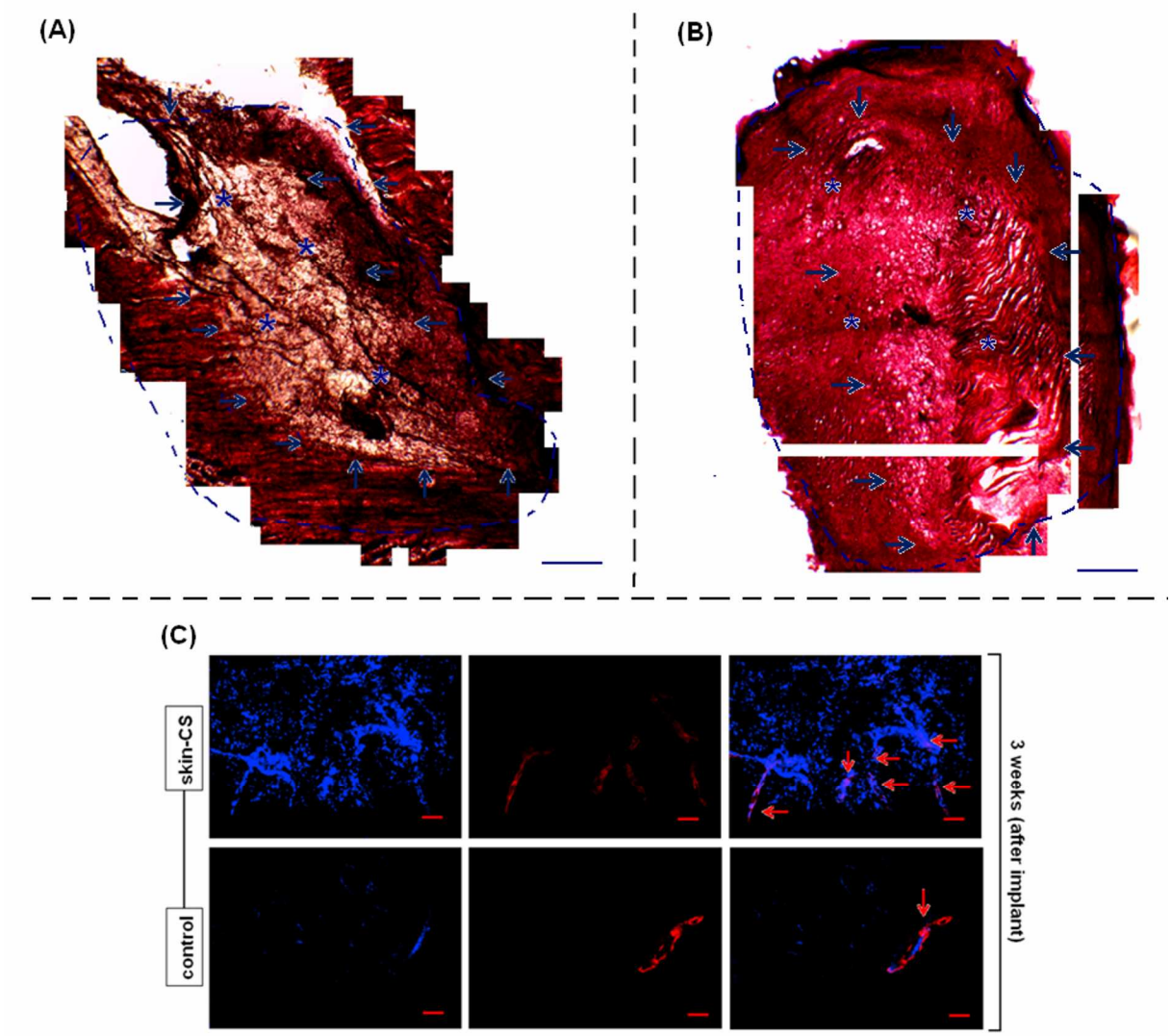

Figure 7 A-C. 3 weeks implants analysis. After 21 days, the natural skin regeneration process was observed (A, stars indicate the new tissue and arrows the limit of the excision); however, the skin-CS implants reported a new-formed tissue more compact and thick (B) more similar to the naïve one. Furthermore, the skin-CS regions showed a more complete vessels network (C) than the controls. Bar scale=200μm.

4.5. CONCLUSIONS.

In this fourth part of the Thesis, it was demonstrated the regenerative potency of the cell sheet (CS) technology for skin repair. In vivo 3rd degree burn defects were successfully repaired in 1 week, while after 3 weeks a dense and high-vascularized tissue was formed. The skin-CS induced repair was more effective and fast than the natural one. The CS was even improved by the introduction of the elastin layer as scaffold for cells, showing how the CS technique represent a suitable tool for further improvements in order to expand the use of CS for the treatment of other tissues.

Acknowledgments.

A. Cochis would like to thanks Dr. Enrico Catalano for the excellent assistant for the *in vitro* characterizations and to Dr. Elena Varoni for the help for the *in vivo* surgical procedures. A special thanks to Prof. Antonella Bandiera (University of Trieste) for producing and providing HELP raw material and all the chemicals (enzymes and specific antibody) necessary for HELP-hydrogel characterizations.

References.

1. Midwood KS, Williams LV, Schwarzbauer JE. Tissue repair and the dynamics of the extracellular matrix. Int J Biochem Cell Biol. 2004;36:1031–7.
2. Mascre´ G, Dekoninck S, Drogat B, et al. Distinct contribution of stem and progenitor cells to epidermal maintenance. Nature. 2012;489:257–62.
3. De Rosa L, De Luca M. Cell biology: dormant and restless skin stem cells. Nature. 2012;489:215–7.
4. Blanpain C, Lowry WE, Geoghegan A, et al. Selfrenewal, multipotency, and the existence of two cell populations within an epithelial stem cell niche. Cell. 2004;118:635–48.
5. Diegelmann RF, Evans MC. Wound healing: an overview of acute, fibrotic and delayed healing. Front Biosci. 2004;9:283–9.
6. Shevchenko RV, James SL, James SE. A review of tissue-engineered skin bioconstructs available for skin reconstruction. J R Soc Interface. 2010;7:229–58.
7. Zilberman M, Elsner JJ. Antibiotic-eluting medical devices for various applications. J Control Release. 2008;130:202–15.
8. Wolfe RA, Roi LD, Flora JD, et al. Mortality differences and speed of wound closure among specialized burn care facilities. JAMA. 1983;250:763–6.
9. Cardinal M, Eisenbud DE, Armostrong DG, et al. Serial surgical debridement: a retrospective study on clinical outcomes in chronic lower extremity wounds. Wound Repair Regen. 2009;17:306–11.
10. Halim AS, Khoo TL, Mohd Yussof SJ. Biologic and synthetic skin substitutes: an overview. Indian J Plast Surg. 2010;43:23–8.
11. Catalano E, Cochis A, Varoni E, et al. Tissue-engineered skin substitutes: an overview. J Artif Organs DOI 10.1007/s10047-013-0734-0.
12. Kroner E, Kaiser JS, Fischer SC, et al. Bioinspired polymeric surface patterns for medical applications. J Appl Biomater Funct Mater. 2012;10:287–92.
13. An initial evaluation of the safety and activity of Celaderm (TM) treatment regimens in healing venous leg ulcers. Clinical trial from Shire Regenerative Medicine, Inc. U.S. National Institutes of Health (January 19, 2012) NCT00399308.
14. Gordley K, Cole P, Hicks J, et al. A comparative, long term assessment of soft tissue substitutes: AlloDerm, Enduragen, and Dermamatrix. J Plast Reconstr Aesthet Surg. 2009;62:849–50.
15. Mansbridge J. Commercial considerations in tissue engineering. J Anat. 2006;209:527–32.
16. Ackermann K, Lombardi Borgia S, Korting H, et al. The Phenion full-thickness skin model for percutaneous absorption testing. Skin Pharmacol Physiol. 2010;23:105–12.
17. Stark HJ, Boehnke K, Mirancea N, et al. Epidermal homeostasis in long-term scaffold enforced skin equivalents. J Investig Dermatol Symp Proc. 2006;11:93–105.
18. Ponec M, El Ghalbzouri A, Dijkman R, et al. Endothelial network formed with human dermal microvascular endothelial cells in autologous multicellular skin substitutes. Angiogenesis. 2004;7:295–305.
19. Erdag G, Morgan JR. Allogenic versus xenogenic immune reaction to bioengineered skin grafts. Cell Transplant. 2014;13:701-12.
20. Urry, DW; Long MM; Cox BA; et al. The synthetic polypentapeptide of elastin coacervates and forms filamentous aggregates. Biochim Biophys Acta. 1974;371:597–602.
21. Bandiera A; Taglienti A; Micali F; et al. Expression and characterization of human-elastin-repeat-based temperature-responsive protein polymers for biotechnological purposes. Biotechnol Appl Biochem. 2005;42:247–56.
22. Ma B, Xie J, Jiang J, et al. Sandwich-type fiber scaffolds with square arrayed micro-wells and nanostructured cues as microskin grafts for skin regeneration. Biomaterials. 2014;35:630-41.